
Louisiana Transportation Research Center

Final Report 578

Roller Compacted Concrete over Soil Cement under Accelerated Loading

by

Zhong Wu
Tyson Rupnow
Moinul I. Mahdi

LTRC



4101 Gourrier Avenue | Baton Rouge, Louisiana 70808
(225) 767-9131 | (225) 767-9108 fax | www.ltrc.lsu.edu

TECHNICAL REPORT STANDARD PAGE

| | | | |
|---|--------------------------------------|--|----------------------------|
| 1. Report No. FHWA/LA.16/578 | | 2. Government Accession No. | 3. Recipient's Catalog No. |
| 4. Title and Subtitle Roller Compacted Concrete over Soil Cement under Accelerated Loading | | 5. Report Date June 2017 | |
| | | 6. Performing Organization Code LTRC Project Number: 12-7P | |
| 7. Author(s) Zhong Wu, Tyson Rupnow, and Moinul I. Mahdi | | 8. Performing Organization Report No. | |
| 9. Performing Organization Name and Address Department of Civil and Environmental Engineering Louisiana State University Baton Rouge, LA 70803 | | 10. Work Unit No. 12-7P | |
| | | 11. Contract or Grant No. | |
| 12. Sponsoring Agency Name and Address Louisiana Department of Transportation and Development P.O. Box 94245 Baton Rouge, LA 70804-9245 | | 13. Type of Report and Period Covered Final Report May 2012-December 2016 | |
| | | 14. Sponsoring Agency Code | |
| 15. Supplementary Notes Conducted in Cooperation with the U.S. Department of Transportation, Federal Highway Administration | | | |
| 16. Abstract In this study, six full-scale APT pavement sections, each 71.7 ft. long and 13 ft. wide, were constructed at the LTRC's Pavement Research Facility (PRF) using normal pavement construction procedures. The test sections include three RCC thicknesses (4 in., 6 in., and 8 in.) and two base designs: a 150 psi unconfined compressive strength (UCS) cement treated soil base with a thickness of 12 in. and a 300 psi UCS soil cement base with a thickness of 8.5 in. over a 10 in. cement treated subgrade. A heavy vehicle load simulation device (ATLaS30) was used for APT loading. In situ pavement testing, instrumentation, and crack-mapping were employed to monitor the load-induced pavement responses and pavement cracking performance. The APT results generally indicated that a thin RCC pavement (thickness of 4 to 6 in.) would eventually have a structurally fatigue cracking failure under the repetitive traffic and environmental loading due to a combined effect of pavement cracking and pumping. The visible cracks first showed up on pavement surface as a single or several fine cracks along the longitudinal traffic direction within the wheel paths. The longitudinal cracks were then extended and gradually propagated to transverse and other directions under the continued loading, and finally merged into a fatigue cracking failure. Post-mortem trenching results showed that the majority of the cracks were bottom-up, but some did show developed as the top-down. The results further showed that all tested thin RCC pavement structures over an adequate base support would have superior load carrying capability. The 6-in. RCC sections carried an estimated 87.4 million and 19.4 million ESALs to failure for the soil cement and cement treated base, respectively. The 4-in. RCC section over the soil cement base performed well with an estimated 19.2 million ESALs to failure. The data also indicated that the more substantial base (i.e., soil cement) support generally provided additional structural capacity as compared the less substantial cement treated soil base. The APT results were then used to evaluate the pavement fatigue life, cracking pattern and failure mode of thin RCC-surfaced pavements, which led to the development of a set of RCC fatigue models for thin RCC fatigue damage analysis. Finally, a thickness design procedure that includes a fatigue model suitable for analyzing a thin RCC surfaced pavement structure was proposed and the corresponding construction cost savings when implementing thin RCC-surfaced pavement as a design option for a low volume pavement were estimated. | | | |
| 17. Key Words Roller compacted concrete, cracking, pavement performance, fatigue analysis, thickness design | | 18. Distribution Statement Unrestricted. This document is available through the National Technical Information Service, Springfield, VA 21161. | |
| 19. Security Classif. (of this report) | 20. Security Classif. (of this page) | 21. No. of Pages | 22. Price |

Project Review Committee

Each research project will have an advisory committee appointed by the LTRC Director. The Project Review Committee is responsible for assisting the LTRC Administrator or Manager in the development of acceptable research problem statements, requests for proposals, review of research proposals, oversight of approved research projects, and implementation of findings.

LTRC appreciates the dedication of the following Project Review Committee Members in guiding this research study to fruition.

LTRC Administrator/Manager

Zhongjie “Doc” Zhang, Ph.D., P.E.
Pavement and Geotechnical Research Administrator

Members

Jeff Lambert, DOTD
John Eggers, DOTD
Bill Temple, CAAL
Jacques Deville, DOTD
Brian Owens, DOTD
Scott Nelson, FHWA

Directorate Implementation Sponsor

Janice P. Williams, P.E.
DOTD Chief Engineer

Roller Compacted Concrete over Soil Cement under Accelerated Loading

by

Zhong Wu
Tyson Rupnow
Moinul I. Mahdi

Louisiana Transportation Research Center
4101 Gourrier Avenue
Baton Rouge, LA 70808

LTRC Project No. 12-7P
State Project No. 30000682

conducted for

Louisiana Department of Transportation and Development
Louisiana Transportation Research Center

The contents of this report reflect the views of the author/principal investigator who is responsible for the facts and the accuracy of the data presented herein. The contents do not necessarily reflect the views or policies of the Louisiana Department of Transportation and Development, the Federal Highway Administration or the Louisiana Transportation Research Center. This report does not constitute a standard, specification, or regulation.

June 2017

ABSTRACT

Thin Roller Compacted Concrete (RCC) pavement (i.e., the RCC thickness < 8 in.) has drawn a great deal of attention in recent years due to its potential application for low volume roadways where heavy and/or overloaded truck trafficking are often encountered. However, neither a structural design procedure nor load-induced pavement fatigue damage analysis is currently available for a thin RCC-surfaced pavement thickness design. The objectives of the study were to determine the structural performance and load carrying capacity of thin RCC-surfaced pavements under accelerated pavement testing (APT), and to determine the applicability of using a thin RCC pavement structure with cement treated or stabilized base as a design alternative for those low volume roadways having frequently heavy truck trafficking.

In this study, six full-scale APT pavement sections, each 71.7 ft. long and 13 ft. wide, were constructed at the LTRC's Pavement Research Facility (PRF) using normal pavement construction procedures. The test sections include three RCC thicknesses (4 in., 6 in., and 8 in.) and two base designs: a 150 psi unconfined compressive strength (UCS) cement treated soil base with a thickness of 12 in. and a 300 psi UCS soil cement base with a thickness of 8.5 in. over a 10 in. cement treated subgrade. A heavy vehicle load simulation device - ATLaS30 was used for APT loading. In-situ pavement testing, instrumentation, and crack-mapping were employed to monitor the load-induced pavement responses and pavement cracking performance.

The APT results generally indicated that a thin RCC pavement (thickness of 4 to 6 in.) would eventually exhibit structural fatigue cracking failure under the repetitive traffic and environmental loading due to a combined effect of pavement cracking and pumping. The visible cracks first showed up on pavement surface as a single or several fine cracks along the longitudinal traffic direction within the wheel paths. The longitudinal cracks were then extended and gradually propagated to transverse and other directions under the continued loading, and finally merged into a fatigue cracking failure. Post-mortem trenching results showed that the majority of the cracks were bottom-up, but some did show developed as the top-down.

The results further showed that all tested thin RCC pavement structures over an adequate base support would have superior load carrying capability. The 6-in. RCC sections carried an estimated 87.4 million and 19.4 million ESALs to failure for the soil cement and cement treated base, respectively. The 4-in. RCC section over the soil cement base performed well

with an estimated 19.2 million ESALs to failure. The data also indicated that the more substantial base (i.e., soil cement) support generally provided additional structural capacity as compared the less substantial cement treated soil base. The APT results were then used to evaluate the pavement fatigue life, cracking pattern and failure mode of thin RCC-surfaced pavements, which led to the development of a set of RCC fatigue models for thin RCC fatigue damage analysis. Finally, a thickness design procedure that includes a fatigue model suitable for analyzing a thin RCC-surfaced pavement structure was proposed and the corresponding construction cost savings when implementing thin RCC-surfaced pavement as a design option for a low-volume pavement were estimated.

ACKNOWLEDGMENTS

This study was supported by the Louisiana Transportation Research Center (LTRC) and the Louisiana Department of Transportation and Development (DOTD) under LTRC Research Project Number 12-7P. The authors would like to express thanks to all those who provided valuable help in this study.

IMPLEMENTATION STATEMENT

The accelerated pavement testing experiment of this study demonstrated in a field environment that a thin RCC (i.e., the slab thickness of 4 to 6 in.) over a soil cement or cement treated base pavement structure can provide a cost-effective and durable pavement design option for low-volume roads in Louisiana where heavy and/or overloaded trucks are often encountered. In fact, the results showed that a thin RCC-surfaced over soil cement pavement structure has a superior load carrying capability. In addition, a stronger pavement foundation (i.e., soil cement over a treated subgrade) generally provided additional structural capacity that may be equivalent to a 2-in. thickness of RCC as compared to a less substantial foundation used (i.e., a thin RCC slab directly built over a cement treated base). Therefore, the researchers recommend that DOTD consider implementing a thin RCC-surfaced pavement structure as a pavement design alternative in low-volume pavement design. The recommended pavement structure consists of a thin RCC slab (usually 4~6 in.) built over a soil cement or cement treated base layer. The pavement structural design may follow the thickness design procedure provided in this study. The designed RCC mixes shall have similar material composition and gradation as those of this study, but using more fine aggregates and natural sands to achieve a better RCC roadway density and smoother pavement surface (e.g., IRI = 100~120 in/mile). If the RCC pavement shall be used for high-volume roadways, a thin asphalt overlay or surface diamond grinding may be needed to provide a better pavement surface ridability.

TABLE OF CONTENTS

| | |
|---|-----|
| ABSTRACT..... | iii |
| ACKNOWLEDGMENTS | v |
| IMPLEMENTATION STATEMENT | vi |
| TABLE OF CONTENTS..... | vii |
| LIST OF TABLES..... | ix |
| LIST OF FIGURES | xi |
| INTRODUCTION | 1 |
| Summary of Literature..... | 1 |
| RCC Engineering Properties..... | 1 |
| RCC Mixture Design | 3 |
| RCC Pavement Design | 4 |
| RCC Pavement Performance | 6 |
| Previous Studies on RCC Pavements | 7 |
| OBJECTIVE | 11 |
| SCOPE | 13 |
| METHODOLOGIES | 15 |
| Description of APT Test Sections..... | 15 |
| Pavement Structures..... | 15 |
| Materials | 16 |
| Construction of APT Test Sections..... | 18 |
| Instrumentation | 21 |
| Accelerated Loading Experiment | 26 |
| APT Loading Device | 26 |
| Failure Criteria and Loading History | 27 |
| Field Measurements and Non-Destructive Testing..... | 28 |
| Data Analysis Techniques..... | 29 |
| DISCUSSION OF RESULTS..... | 31 |
| Results from Laboratory Tests..... | 31 |
| RCC Mix Design..... | 31 |
| RCC Used in Test Lanes..... | 34 |
| Results from RCC APT Test Sections | 36 |
| Surface Characteristics and In-Situ Density | 36 |
| Slab Thicknesses and Backcalculated Layer Moduli..... | 38 |
| Typical Instrumentation Responses | 40 |
| Performance of RCC APT Sections..... | 43 |

| | |
|---|----|
| Post-Mortem Trenches..... | 44 |
| Prediction of Field Tensile Stress and FEA..... | 45 |
| Analysis of Cracking Potentials of Thin RCC Pavements..... | 47 |
| Fatigue Cracking and Failure Mechanism on Thin RCC Pavements..... | 51 |
| Procedure for Thin RCC Pavement Design..... | 52 |
| Design Period and Traffic Inputs..... | 53 |
| Failure Criteria..... | 53 |
| Design Spreadsheet..... | 57 |
| Design Example..... | 58 |
| Construction Cost Analysis..... | 61 |
| CONCLUSIONS..... | 63 |
| RECOMMENDATIONS..... | 65 |
| ACRONYMS, ABBREVIATIONS, AND SYMBOLS..... | 67 |
| REFERENCES..... | 69 |
| APPENDIX A..... | 71 |
| Loading Sequence..... | 71 |
| Section 6 (4+8.5RCC)..... | 72 |
| Section 5 (6+8.5RCC)..... | 74 |
| Section 3 (4+12RCC)..... | 75 |
| Section 2 (6+12RCC)..... | 76 |
| Section 4 (8+8.5RCC)..... | 77 |
| APPENDIX B..... | 79 |

LIST OF TABLES

| | |
|--|----|
| Table 1 Recent thin RCC projects around United States | 9 |
| Table 2 Basic soil properties..... | 17 |
| Table 3 APT loading passes and load magnitudes..... | 28 |
| Table 4 Sand patching and DFT test results | 37 |
| Table 5 Nuclear density test results for RCC test sections | 38 |
| Table 6 Thickness variation of RCC sections..... | 39 |
| Table 7 Field measured and predicted responses of RCC test sections..... | 47 |
| Table 8 Example load distribution of traffic axle loads..... | 59 |
| Table 9 Fatigue and erosion analysis results for proposed design..... | 60 |
| Table 10 Initial construction costs | 62 |

LIST OF FIGURES

| | |
|--|----|
| Figure 1 Comparison between RCC and PCC mixtures..... | 4 |
| Figure 2 RCC shoulder construction in Georgia (I-285) | 8 |
| Figure 3 RCC travel lane construction in South Carolina (U.S. 78) | 9 |
| Figure 4 RCC test sections..... | 15 |
| Figure 5 Combined gradation results for the proposed aggregate combination | 16 |
| Figure 6 Combined gradation results for proposed aggregate combination | 16 |
| Figure 7 Seven-day unconfined compressive strength for different cement content..... | 17 |
| Figure 8 Construction of RCC test sections..... | 20 |
| Figure 9 In-Situ sample fabrication | 21 |
| Figure 10 Instrumentation plan..... | 22 |
| Figure 11 TDR calibration..... | 24 |
| Figure 12 Instrumentation of RCC test sections | 25 |
| Figure 13 The ATLaS30 device..... | 26 |
| Figure 14 The measured tire prints under different loads..... | 27 |
| Figure 15 In-Situ and non-destructive testing..... | 29 |
| Figure 16 Moisture density relationship for 350 pcy cement content mixture | 31 |
| Figure 17 Moisture density relationship for 400 pcy cement content mixture | 32 |
| Figure 18 Moisture density relationship for 450 pcy cement content mixture | 32 |
| Figure 19 Moisture density relationship for 500 pcy cement content mixture | 33 |
| Figure 20 Compressive strength results for all mixtures | 34 |
| Figure 21 Average compressive strength results for samples produced for Lane 1 and 2 | 35 |
| Figure 22 Surface texture of the constructed test sections..... | 36 |
| Figure 23 One-point Proctor specimen | 38 |
| Figure 24 FWD backcalculated moduli of RCC test sections | 40 |
| Figure 25 Typical Instrumentation response under ATLaS 30 loading..... | 41 |
| Figure 26 Comparison of load-induced pavement responses grouped by: (a) RCC thickness, (b) different bases..... | 42 |
| Figure 27 Typical temperature and moisture responses | 42 |
| Figure 28 RCC pavement condition at the end of testing..... | 43 |
| Figure 29 Bottom-up longitudinal cracking and voids under the wheel path..... | 44 |
| Figure 30 Top-down longitudinal cracks within and outside the wheel path..... | 45 |
| Figure 31 Cracks at the saw-cutting joint | 45 |
| Figure 32 RCC pavement structures used in finite element analysis..... | 46 |
| Figure 33 Relative locations of nodes and tire print in the finite difference model | 48 |
| Figure 34 Maximum flexural stresses versus the distance of loading from joint | 49 |

| | |
|---|----|
| Figure 35 Maximum flexural stresses versus the length of the slab | 50 |
| Figure 36 Maximum flexural stresses versus length of separation zone | 51 |
| Figure 37 The flowchart of the proposed thin RCC design procedure | 58 |
| Figure 38 Pavement alternatives used in cost-benefit analysis..... | 61 |
| Figure 39 Loading sequence and corresponding ESALs for Section 6 (4+8.5RCC) | 71 |
| Figure 40 Cracks vs. load repetitions for Section 6 (4+8.5RCC) | 72 |
| Figure 41 Distresses observed on Section 6 (4+8.5RCC) | 73 |
| Figure 42 Cracks vs. load repetitions for Section 5 (6+8.5RCC)..... | 74 |
| Figure 43 Distresses observed on Section 5 (6+8.5RCC) | 75 |
| Figure 44 Cracks vs. load repetitions for Section 3 (4+12 RCC)..... | 75 |
| Figure 45 Cracks vs. load repetitions for Section 2 (6+12 RCC) | 77 |

INTRODUCTION

Roller compacted concrete is a zero-slump concrete mixture placed with high density asphalt paving equipment and compacted by vibratory rollers [1]. RCC has similar strength properties and consists of the same basic ingredients as conventional concrete—well-graded aggregates, cementitious materials, and water—but has different mixture proportions. Properly designed RCC mixes can achieve outstanding compressive strengths similar to those of conventional concrete. The major difference between RCC mixtures and conventional concrete mixtures is that RCC has a higher percentage of fine aggregates, which allows for tight packing and consolidation. Due to its relatively coarse surface, RCC has traditionally been used for pavements carrying heavy loads in low-speed areas, such as parking, storage areas, port, airport service areas, intermodal, and military facilities [1]. With improved paving and compaction methods as well as surface texturing techniques, recent applications of RCC are found for interstate highway shoulders, city streets, and other highways [2-5].

RCC is an economical, fast and durable candidate for many pavement applications. The proven durability and high-load carrying capacity of RCC, combined with its simple and cost-effective construction method and high placement speed, has created a great deal of interest from many state and local transportation agencies. Traditionally RCC pavements have been built that are on the order of 8 to 12+ in. thick. With the increasing shale gas exploration, agricultural activities, and logging activities on the low-volume roadways, the Louisiana Department of Transportation and Development (DOTD) and the Louisiana Transportation Research Center (LTRC) are interested in thin applications of RCC to be used a design alternative for those low-volume roadways having frequently heavy truck trafficking.

Summary of Literature

RCC Engineering Properties

The properties of RCC are similar to those of conventional concrete pavement but are achieved using different mixture proportions and construction techniques. Generally, the aggregate skeleton of RCC mixes is comprised of fine aggregate and coarse aggregate. The nominal maximum size is usually limited to $\frac{3}{4}$ in. in order to reduce the potential for segregation during production and placement and limiting the maximum size of aggregate also facilitates placement operations and improves surface texture. As with conventional concrete, fine aggregates can consist of natural sand, manufactured sand, or a mixture of both [6].

The compressive strength of RCC typically ranges from 4,000 to 6,000 psi. Some projects have reached compressive strengths higher than 7,000 psi. However, practical construction and cost considerations would likely specify increased thickness rather than strengths of this nature. The densely graded aggregate structures in RCC mixtures help the concrete achieve high levels of compressive strength. The low water cement ratio (w/c) of RCC mixtures produces a low-porosity cement matrix that also contributes to the high compressive strength of the concrete. Every mixture proportion has an optimum moisture content at which it achieves the maximum dry density. This density most often provides the maximum strength.

Flexural strength is directly related to the density and compressive strength of the concrete mixture. In properly constructed RCC pavements, the aggregates are densely packed and minimize the development of fatigue cracking. The density of the paste and the strength of its bond to the aggregate particles are high due to its low w/ cm ratio. As a result, the flexural strength of RCC, depending on the mix design, is generally high, ranging from 500 to 1,000 psi.

The modulus of elasticity represents the material's propensity to undergo reversible elastic deformation in response to a stress. Field core results indicate that the moduli of elasticity of RCC mixtures are similar to or slightly higher than those of conventional concrete when the mixtures have similar cement contents [6].

Fresh RCC is stiffer than typical zero-slump conventional concrete. Its consistency is stiff enough to remain stable under vibratory rollers, yet wet enough to permit adequate mixing and distribution of paste without segregation. The strength properties of RCC depend on the amount of cementations materials, w/c, quality of aggregates, and degree of compaction of the concrete. In general, RCC pavements can achieve compressive and flexural strengths comparable or exceeding to those of conventional concrete pavements. Mix design analysis is conducted as necessary to meet design strength criteria [1].

Tests commonly used to determine RCC engineering properties include the following:

- ASTM C1435 / C1435M, Standard Practice for Molding Roller-Compacted Concrete in Cylinder Molds Using a Vibrating Hammer.
- ASTM D1557, Standard Test Methods for Laboratory Compaction Characteristics of Soil Using Modified Effort (56,000 ft-lbf/ft³ [2,700 kN-m/m³]).
- ASTM C39 / C39M, Standard Test Method for Compressive Strength of Cylindrical Concrete Specimens.

- ASTM C42 / C42M, Standard Test Method for Obtaining and Testing Drilled Cores and Sawed Beams of Concrete.
- Vebe Testing ASTM C1170 / C1170M, Standard Test Method for Determining Consistency and Density of Roller-Compacted Concrete Using a Vibrating Table.
- ASTM C78, Standard Test Method for Flexural Strength of Concrete (Using Simple Beam with Third-Point Loading).

RCC Mixture Design

RCC mixture design is different from the design methods generally used for conventional concrete (Figure 1). The most commonly used methods for designing RCC mixes are described in the American Concrete Institute's (ACI) Committee 325.10R-95, which provides two design methods: the method based on workability limits and the method based on geotechnical principles. The U.S. Army Corps of Engineers (USACE) and Portland Cement Association (PCA) design procedures are similar to the ACI's first and second methods, respectively [7-8]. The ACI methods are empirically-based. The "workability method" is through determining a suitable water-cement ratio and sand-binder ratio to produce RCC mixes with a target workability limit; whereas, the "geotechnical principle method" is to determine the proportion of RCC mixes through a soil compaction procedure based on the relationship between RCC dry density and water content. RCC mixes can be also designed based on the semi-empirical methods (e.g., the optimal paste volume method) or the theoretical methods (e.g., the Compressible Packing Model). The optimal paste volume method is based on the hypothesis that the optimal RCC mix should have just enough paste to fill the inter-granular spaces remaining after the aggregate skeleton has achieved maximum [1]. The Compressible Packing Model, developed by the Laboratoire Central des Ponts et Chaussées (LCPC) in France, has been particularly effective in designing concrete mixes with optimal aggregate compactness based on optimizing the packing of different-sized particles to control the porosity of RCC. The method, therefore, makes it possible to combine constituents to produce a dry mix with optimal compactness for a given workability. Recently, a Superpave gyratory compaction-based RCC design method has been introduced, which can be used to select the appropriate cement content to deliver the required strength for a specific RCC pavement project [6].

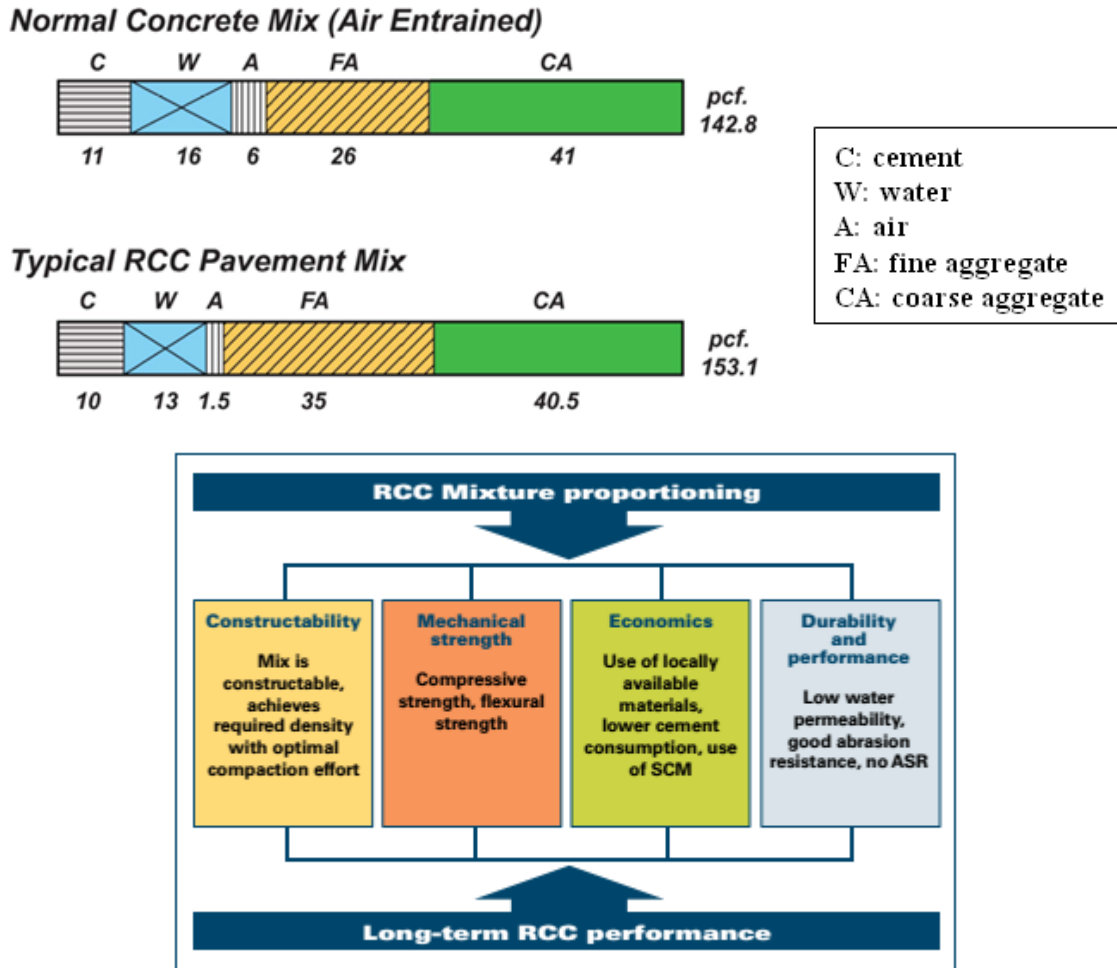


Figure 1
Comparison between RCC and PCC mixtures

RCC Pavement Design

RCC pavement design methods employ the same basic strategy as for conventional concrete pavements: keeping the pavements flexural stress and fatigue damage caused by wheel loads within allowable limits. The RCC layer thickness is a function of expected loads, concrete strength (modulus of rupture), and soil characteristics. The calculations for determining the thickness of RCC pavements are based on three general principles.

Thickness design procedures for RCC pavements for heavy industrial applications (such as ports and multimodal terminals) have been developed by the PCA and USACE [7-8]. The design approach involves the assumption that the pavement structure can withstand loads of certain magnitudes at certain repetition levels without failing. Because the critical stresses in RCC are flexural, fatigue due to flexural stress is usually used in the thickness design.

Fatigue failure occurs when a material is subjected to repeated stresses. While the stress caused by a single load is not greater than the strength of the material (and therefore will not cause the material to fail), repetition of these loads will wear on the material over time and eventually result in fatigue failure. In addition, the PCA method also considers the erosion criterion in RCC thickness design. This criterion limits the erosion of materials underlying the pavement caused by deflections resulting from repeated loading along edges and joints (pumping). It can also control faulting at joints and deterioration of shoulders. Critical deflection occurs at the slab corner when the load is applied near the joint.

The general thickness design principle based on the fatigue criterion is to set the RCC pavement thickness from the outset. Stresses at the top and bottom of the pavement (depending on loading) are then calculated for every category (i) of axial load. The maximum number of repetitions (N_i) for each load category (pavement fatigue capacity) is determined as a function of the ratio between the concrete's (σ) stress and modulus of rupture (MR). The percentage of the pavement fatigue capacity used by each load category in the design period is equal to the ratio of the number of expected repetitions (n_i) and the maximum allowable number of repetitions (N_i). The cumulative damage caused to the pavement by fatigue, D_f , is given by the following relationship, where j represents the total number of load categories in the design period:

$$D_f = \sum_{i=1}^j \frac{n_i}{N_i} \quad (1)$$

The cumulative damage at the end of the design period must be less than or equal to 1. If the sum of the damage is greater than 1, the process must be repeated with a thicker RCC pavement until $D \leq 1$. When using the PCA method in a RCC pavement design, slab thickness and modulus of rupture are predominant factors in the design life of RCC pavements. However, both design procedures are mostly applicable for RCC pavements for heavy industrial applications (such as ports and multimodal terminals) with a minimum design RCC thickness of 8 in. [2]. The PCA procedure was later incorporated into a computer program called RCC-PAVE. The following fatigue model in equation (2) is used in RCC-PAVE [9]:

$$\text{Log } N_f = 10.25476 - 11.1872 (\text{SR}) \quad \text{for } \text{SR} > 0.38 \quad (2)$$

Meanwhile, equation (3) shows the fatigue model used for PCC pavement thickness design developed by American Concrete Institute (ACI) [10]:

$$N_f = (4.2577 / (\text{SR} - 0.4325))^{3.268} \quad \text{for } 0.45 < \text{SR} < 0.55$$

$$\text{Log Nf} = 11.737 - 12.077 (\text{SR}) \quad \text{for } \text{SR} \geq 0.55 \quad (3)$$

where,

Nf = the allowable number of load repetitions

SR = Stress Ratio, critical (maximum) flexural stress under wheel loads divided by flexural strength of the concrete slab.

ACPA's intent is to develop a RCC fatigue curve based on available published RCC fatigue data and include a reliability component to improve thickness design. The new ACPA RCC fatigue model is being proposed as a replacement to the current RCC Design Curve published by CTL in 1987. It represents a significant improvement to the RCC thickness design by using all available RCC fatigue data and removing arbitrary assumptions used to develop the past model.

RCC Pavement Performance

Properly designed RCC pavements can achieve strength properties equal or exceeding to those of conventional concrete with very low permeability. Cracks will develop in an RCC pavement slab as a natural result of the shrinkage process during curing. These cracks would normally occur on a random basis every 30 to 90 ft. Because there is no bleed water in RCC, there is less shrinkage cracking than that occurs with conventional PCC. The shrinkage cracks that occur in RCC pavements are usually small (less than 0.1-in.) and very good load transfer exists across the crack through aggregate interlock. This aggregate interlock is enhanced through the use of the dense-graded aggregate structure specified for RCC mixtures. Long-term performance studies of RCC pavements have shown almost no evidence of crack faulting (the vertical displacement of the pavement slab at the crack), which provides further indication of the load transfer provided by aggregate interlock [2].

RCC pavements have shown to require very little maintenance. Cracks are sometimes routed and sealed, but usually crack spalling is not a significant problem. The most common type of repair occurs with small areas where the RCC may have been placed by hand, or around structures. In these locations, if the RCC is not satisfactory, it can be removed and replaced with a repair using conventional concrete.

RCC pavements have been reported to be cheaper than both conventional concrete and asphalt pavements. The Tennessee Department of Transportation (DOT) found that the cost per square yard or meter for RCC was 84% of the cost of state-constructed asphalt pavement and 62% of the cost of an in-place bid for contractor-placed asphalt [11]. In Canada, the Dufferen Construction Company has found that the in-place cost per cubic yard/ cubic meter

of RCC is 89% that of asphalt and 62% that of 3,600 psi compressive strength conventional portland cement concrete pavement [12].

However, RCC pavements are not as smooth as conventional PCC pavements. The pavement roughness (i.e., riding comfort) has long limited RCC applications for which vehicle speed is an important factor. Riding comfort is estimated from the positive or negative variations of the pavement with respect to a level surface. Pavement roughness is affected by longitudinal and transversal undulations, as well as, the length of vertical deformations. RCC pavement roughness is significantly affected by construction procedures, variations in degree of compaction, uniformity of placement by the paver, and compaction operations. High-density pavers have significantly improved the uniformity of RCC pavements. Projects have been successfully constructed using a 0.2-in. straight-edge tolerance when measuring the pavement surface using a 10-ft. straight-edge. If pavement smoothness is particularly important for a RCC project, the following steps can be taken to improve the final results:

- Use a maximum aggregate size no larger than 0.5-in.
- Do not construct the pavement in layers exceeding 8-in. in thickness (after compaction)
- Use a high-density paver with string-line grade control
- Achieve compaction without excessive rolling

If high-speed operations are required, a thin (2 to 3 in.) layer of asphalt or bonded concrete can be placed over the RCC slab to provide a smooth travelling surface. Diamond grinding of the RCC surface has also been used successfully, and can provide additional smoothness without the construction of a surface overlay.

Previous Studies on RCC Pavements

RCC applications to public roads began in the mid-1980s with a few, relatively short experimental sections on local roads and residential streets [5]. Since then over a hundred RCC pavements on urban streets and intersections have been completed [3]. The following are typical RCC applications [1]:

- Industrial plant access roads and parking lots
- Truck freight terminals, bulk commodity storage, and distribution centers
- Low-volume urban and rural roads
- Aircraft parking areas
- Military loading zones, forward or rearward bases of operation, and airfields
- Large commercial parking lots
- Roadways in public parks
- Roadways for timber and logging operations

- Highway shoulders
- Temporary travel lanes that must be constructed quickly to divert traffic

Most of these public roads were constructed with thin asphalt overlays for better riding quality compared to the inferior surface texture of RCC [13-14]. However, with improved paving and compaction methods as well as surface texture techniques, recent applications of RCC are found to be used for interstate highway shoulders, city streets, and other highways [2-4]. In addition, due to low water content, RCC pavements have reduced shrinkage and low maintenance costs [5].

Considering these advantages in construction speed, strength, durability, and cost, RCC was selected by the Georgia Department of Transportation (GDOT) in 2005 for the paved shoulder on I-285. An expedient construction on weekends with a single lane closure minimized the impact on the traveling public. The finished shoulder was reported in excellent condition at the time of the short-term performance evaluation (9 months after the construction) with limited defects mainly attributed to construction processes, rather than deterioration of the RCC material [4].



Figure 2

RCC shoulder construction in Georgia (I-285)

In 2009, the South Carolina Department of Transportation (SCDOT) placed a 10-in. thick RCC surfaced pavements on U.S. highway 78 near Aiken, SC. The project consisted of a 4-lane, 1-mile long route of failed asphalt pavement that required rehabilitation or replacement. The repair method chosen consisted of milling out the distressed asphalt and replacing it with 10 in. of RCC. To provide the desired ride quality for high speed traffic SCDOT chose to diamond grind the RCC surface rather than cover it with a thin asphalt or conventional concrete surface. This project marks the first successful completion of diamond grinding RCC pavement for a major road in the United States [2].



Figure 3

RCC travel lane construction in South Carolina (U.S. 78)

RCC utilization has expanded into many other applications such as bike trails, local streets, and roads, commercial parking lots, while continuing to be used in traditional industrial type applications. According to a recent survey conducted by C. Zollinger, between 2011 and 2013, over 172 projects have been paved with RCC covering more than 4.9 million SY (4.1 million SM). Between 2011 and 2013, RCC was placed by 38 different contractors, with 2 contractors paving over 1 million SY (836,127 SM) each, and 11 contractors paving more than 100,000 SY (83,613 SM) each. RCC was placed in 20 different states, with 4 states accounting for 10 projects or more each. As the growth of RCC moves into more states, the number of qualified contractors is also increasing to meet the demand [15]. Table 1 shows some recent thin RCC projects by different states. Once the resources are available, a more detailed literature review and RCC pavement performance on this individual projects will be provided [16].

Table 1

Recent thin RCC projects around United States

| Project Name | Application | State | Year Constructed | RCC Thickness (in.) |
|----------------------------------|--------------------|--------------|-------------------------|----------------------------|
| Grape Creek Road | Local Street | TX | 2011 | 6 |
| Village of Streamwood | Local Street | IL | 2011 | 6 |
| Willow Lane | Local Street | KS | 2011 | NA* |
| Solms Road | Local Street | TX | 2012 | 9 |
| Lake View Heroes Drive | Local Street | TX | 2012 | 6 |
| Hattiesville | Arterial Street | AR | 2012 | 7 and 8 |
| City of Chicago | Local Street | IL | 2012 | 5 |
| Lake View Heroes Dr; 50th Street | Arterial Street | TX | 2012 | 6 |
| Yuma East Wetlands | Local Street | AZ | 2013 | 5 |
| Kay County 44th Street | Arterial Street | OK | 2013 | 5 and 6 |

| | | | | |
|---------------------|-----------------|----|------|---|
| Kay County S Street | Arterial Street | OK | 2013 | 5 |
| Stafford County | Park and Ride | VA | 2014 | 8 |

** Not Available*

OBJECTIVE

The objectives of the study were: (1) to determine the structural performance with failure mechanism and load carrying capacity of thin RCC pavements under accelerated pavement testing, and (2) to determine the applicability of using a thin RCC pavement structure with cement treated or cement stabilized base as a design option for those low-volume roadways having frequently heavy truck trafficking.

SCOPE

To achieve the objectives, an accelerated pavement testing experiment including six full-scale RCC test sections were conducted in this research. The laboratory tests included the mixture design, unconfined compressive strength and flexural strength. In-situ pavement testing program consisted of falling weight deflectometer (FWD) deflection tests, surface texture and profile tests, temperature and load-induced pavement response measurements, crack mapping survey, and forensic trenching. Based on the APT results, a thickness design procedure was developed for thin RCC pavements and potential benefits of using thin RCC pavements were also evaluated.

METHODOLOGIES

Description of APT Test Sections

Pavement Structures

Six RCC pavement test sections were constructed at the Louisiana Pavement Research Facility (PRF) site in Port Allen, Louisiana, using normal highway construction equipment and procedures. Figure 4 presents the plan view and pavement layer thickness configurations of the six test sections. Each section was about 13 ft. wide and 71.5 ft. long. As shown in Figure 4, the pavement structures for Sections 1-3 generally consist of a RCC surface layer (4 to 8 in. thick), a 12-in. cement treated base layer and a natural subgrade; whereas, Sections 4-6 include a RCC surface layer (4 to 8 in. thick), an 8.5-in. soil cement base layer, a 10-in. cement treated subgrade layer and a natural subgrade. DOTD requires that all high-volume pavement design include a treated subgrade layer between the base layer and natural subgrade. The 10-in. cement treated subgrade layer is designed for this purpose. Overall, Sections 1-3 are designed to determine if a thin RCC surface layer can be used as a cost-effective alternative in lieu of asphalt concrete surfacing for low-volume roads having significantly heavy truck traffic; whereas, Sections 4-6 are designed to study the RCC surfacing for high-volume road applications.



| | | |
|--------------------------------|--------------------------------|--------------------------------|
| 8 in. RCC | 6 in. RCC | 4 in. RCC |
| 12 in. Cement Treated Base | 12 in. Cement Treated Base | 12 in. Cement Treated Base |
| Existing Subgrade | Existing Subgrade | Existing Subgrade |
| Section 1 | Section 2 | Section 3 |
| 8 in. RCC | 6 in. RCC | 4 in. RCC |
| 8.5 in. Soil Cement Base | 8.5 in. Soil Cement Base | 8.5 in. Soil Cement Base |
| 10 in. Cement Treated Subgrade | 10 in. Cement Treated Subgrade | 10 in. Cement Treated Subgrade |
| Existing Subgrade | Existing Subgrade | Existing Subgrade |
| Section 4 | Section 5 | Section 6 |

Figure 4
RCC test sections

Materials

Roller Compacted Concrete. The RCC mixture considered in this study includes a type I portland cement, a #67 crushed limestone, and a No. 89 crushed limestone manufactured sand. Figure 5 shows the combined gradation results. The proposed mixture contained 53% coarse aggregate and 47% fine aggregate by weight. Note that this mixture was used in producing the moisture-density specimens. After consulting with the contractor responsible for the mixing and paving operations, a revised mixture was submitted containing 43% coarse and 57% fine aggregate by weight. This provided a denser mixture with a better finished surface texture. This gradation with other design information are shown in Figure 6.

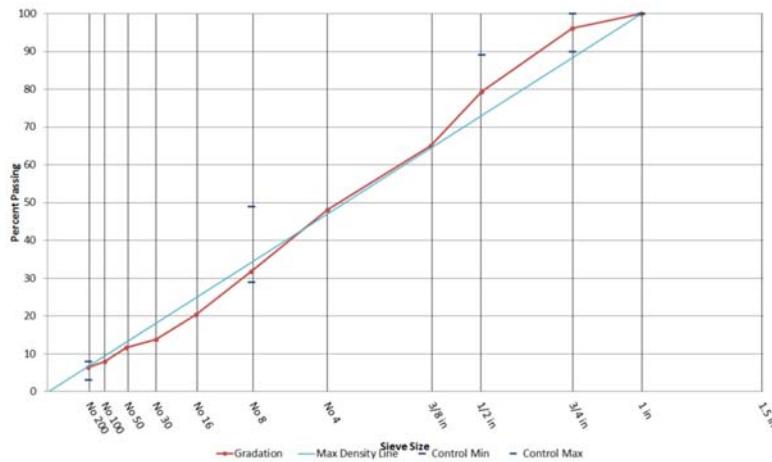


Figure 5

Combined gradation results for the proposed aggregate combination

| Mix Quantities | |
|-------------------------------|-------|
| Max Dry Density (pcf) | 146.0 |
| Max Wet Density (pcf) | 155.5 |
| Optimum % Moisture | 6.5 |
| Coarse Aggregate Absorption % | 0.2 |
| Fine Aggregate Absorption % | 2.1 |
| % Cementitious | 11.4 |
| % Cement | 11.4 |
| % Fly Ash | 0.0 |
| Target Coarse Aggregate % | 45.0 |
| Target Fine Aggregate % | 55.0 |

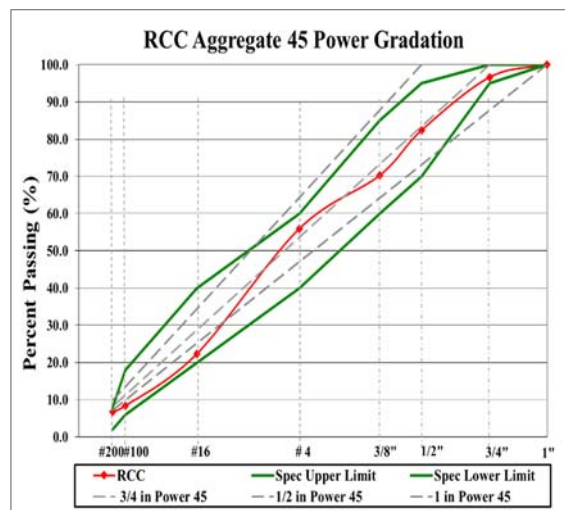


Figure 6

Combined gradation results for proposed revised combination

ASTM D1557 was used for determining the moisture density relationships for each of the mixtures using a manual hammer and a 6-in. diameter mold [17]. ASTM C1435 was used in the preparation of the cylinders for compressive strength [18]. Cylinders were cured in a fog room until testing according to ASTM C39 at 7, 14, and 28-days of age [19].

Base and Subgrade Soils. A silty-clay embankment soil was used in both soil cement and cement treated soil layers as well as the treated subgrade (Table 2). This soil consisted of 47.7% silt and 30% clay. The liquid limit and the plastic index were 32 and 14%, respectively.

Table 2
Basic soil properties

| Class | Clay (%) | Silt (%) | LL (%) | PL | PI | W _{opt} (%) | Density (pcf) |
|-------|----------|----------|--------|----|----|----------------------|---------------|
| A-6 | 30 | 47.7 | 32 | 18 | 14 | 18.5 | 104 |

Figure 7 presents the unconfined compressive strength test results of the A-6 soil with different cement contents. Based on the AASHTO soil classification, it was classified as an A-6 soil. According the DOTD’s roadway design specification, the minimum 7-day unconfined compressive strength for a cement treated soil base and a soil cement base would be 150 and 300 psi, respectively. To meet the specifications, the cement treated soil base layer used in Sections 1-3 contained 6% cement by volume; whereas, 8% by volume of cement was applied in the soil cement base layer on Sections 4-6. On the other hand, a 4% of cement by volume was used for the 10-in. treated subgrade layer on Sections 4-6.

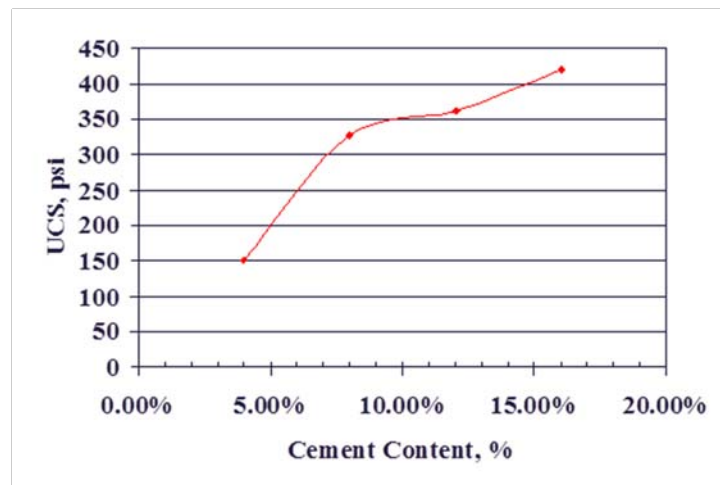


Figure 7
Seven-day unconfined compressive strength for different cement content

Construction of APT Test Sections

The test lane construction for the project was carried out with the assistance from industry partners in the concrete fields using normal highway construction procedures [20]. The Concrete & Aggregates Association of Louisiana (CAAL) was instrumental in arranging industry support through donations to physically construct the test sections. Gilcrest Contractors donated the manpower and equipment necessary to layout and construct the subgrade and base course layers of the RCC test lanes. Rollcon of Houston, Texas also donated their time and their high density paving equipment to construct the test lanes. Cemex donated the manpower to setup and operate the continuous flow pugmill to produce the concrete mixture used in the RCC test lanes.

The construction of the subgrade and base course layers was begun by removing the existing test lanes used in a previous experiment at PRF. The contractor used a Roadtech roto-milling machine to reclaim the existing asphalt pavement. After removing the existing pavements, additional amounts of the subgrade soil (A-6) were added to construct the proposed subgrade layers (Figure 4). Note that a rate of 4% of cement by volume was used to treat the cement treated subgrade layers in Sections 4, 5, and 6. A Caterpillar RM 500 stabilizer was used to process the cement treatment at the plan depth of 10 in. Initial compaction was accomplished by the CP 563 E vibratory sheep foot drum roller, and graded using a CAT motor grader. Final grade was accomplished using a Komatsu D-21P finishing dozer followed by a CAT PS-150C multi-wheel rubber tire roller. A Troxler Nuclear Density gauge was used to measure the field density and moisture right after the construction. In general, the average field proctor density and moisture content for the cement-treated subgrade were 104.5 pcf and 16%, respectively, whereas, for the existing subgrade, the two measurements were 111.3 pcf and 15%, respectively. Subsequently, water was spread on top of the finished subgrade layer for curing. Three PVC pipes were placed at an equal distance to take out all the instrumentation wires through the pipes. Precautions were taken not to damage any wire or PVC pipes during the construction process.

The same procedure was followed for the base layers construction except that a 6% cement by volume was spread for the 12-in. cement treated layer on Sections 1, 2, and 3 and an 8% cement by volume was applied for the 8.5-in. soil cement layer on Sections 4, 5, and 6 to achieve a minimum 7-day UCS of 150 and 300 psi, respectively. Both the base layers were compacted to achieve a 95% of the maximum dry density.

All RCC layers of test sections were constructed within a day using a high density paver and continuous flow pugmill. As shown in Figure 8, the RCC placement involves a number of

steps: RCC production, transportation and placement, compaction, jointing, and curing. For the production of RCC, a Rapidmix 400C horizontal twin shaft pugmill was used. It consists of two aggregate feeders, a cement silo and feeder, a main feeder belt, a water supply system, a pugmill mixer, a discharge belt, and a gob hopper at the end of the discharge belt. The pugmill offers a number of advantages, such as rapid mobilization (takes 2-3 hours from travel mode to fully operational mode), self-contained with its own power source, reduced transportation time for fresh concrete, high production rate (50 to 300 yd^3/hr) and an efficient mixing system [1, 21]. During the startup operation, the pugmill was calibrated and batching of RCC was monitored to fulfill the specification in accordance with ASTM C94. The RCC mix was then transported to the jobsite in dump trucks. Precautions were taken to avoid excessive moisture loss during transportation.

Before placing the RCC on the actual pavement sections, a 200-ft. long trial section was constructed on top of an existing roadway at the PRF site to validate the design, rolling pattern, and method of construction using the same construction equipment. A high density paver was used to place the RCC over the prepared base layer to achieve high initial density and smoother surface. A CAT CB-64 vibratory steel drum roller was then used to achieve finer compaction of the RCC layer. Nuclear density gage was used to check the moisture and density right after the paver and after the compaction using vibratory roller. The density ranges between 94-96 % of the target density right behind the paver and increased to 97-98% after compaction. Note that not all density measurements satisfied the target density value of 98%, but all test sections achieved 96.5% or greater density after the construction.

All RCC layers were placed in single lift and no construction joints were formed. Precautions were taken not to damage any instrumentation wire or PVC pipes during the placement. During the construction, transverse saw-cut joints were created on each RCC test section to minimize or prevent possible randomly-generated shrinkage cracking. Saw-cutting began after RCC was cured enough to withstand spalling damage during sawing operations. The saw-cut joints were typically spaced at 20 ft., 15 ft., and 10 ft. intervals for the 8-in., 6-in., and 4-in. RCC layers, respectively, with the corresponding joint depths of 1.5 in., 1.0 in., and 0.5 in. Finally, a white pigmented water base concrete curing compound conforming to ASTM C309 was sprayed on the finished RCC surfaces for curing.



(a) Rapidmix 400-C Pugmill



(b) Transportation



(c) Placement of RCC



(d) Compaction



(e) Saw-Cutting Joints



(f) Curing

Figure 8
Construction of RCC test sections

Sampling During Construction. LTRC technicians collected cement-stabilized soil materials from the PRF testing sections immediately after they were thoroughly mixed by the stabilizer. The collected mixtures were then brought to LTRC and molded into samples for unconfined compressive strength testing. In addition, as shown in Figure 9, cylindrical samples and saw-cutting beams of RCC were prepared on site during and after construction

for the laboratory strength tests. Several field cylinder cores were also taken from different sections after the construction.



Figure 9
In-Situ sample fabrication

Instrumentation

Figure 10 shows the instrumentation plan of this experiment. Each test section was instrumented with three earth pressure cells (Geokon 3500), two H-type asphalt strain gages (Tokyo Sokki KM-100HAS), and two concrete strain gages (Tokyo Sokki PML-60), which were placed at various locations and layer interfaces. Several moisture sensors (TDR CS 616) and thermocouples (T 108-L) from Campbell Scientific were also placed to monitor the pavement temperature and subgrade moisture variation. The purpose of the instrumentation is to measure the direct pavement responses under the wheel and environmental loading and to provide information for characterization and evaluation of the relative damage evolution of RCC pavements.

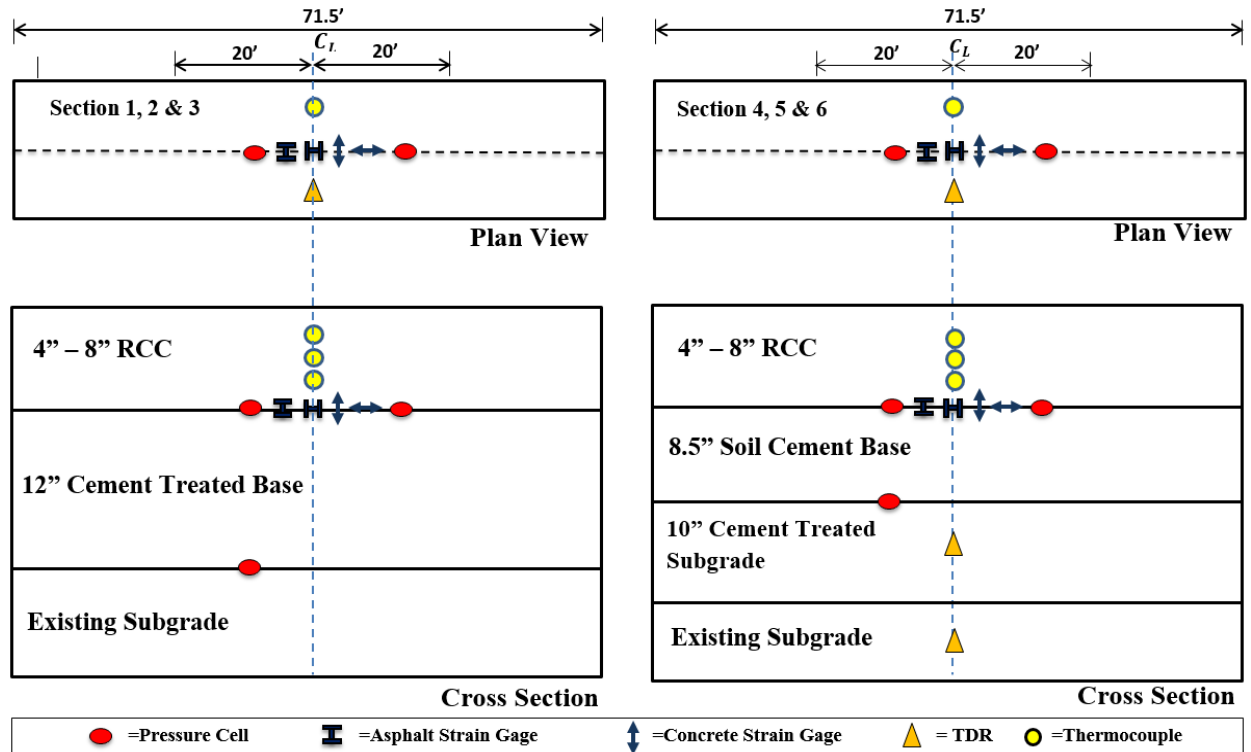


Figure 10
Instrumentation plan

Geokon 3500 Pressure Cell. The Geokon 3500 earth pressure cell, which utilizes a semiconductor pressure transducer as its basic sensing element, has a diameter of 9 in. (229 mm) and a thickness of 0.24 in. (6 mm). Due to having a larger diameter, the Geokon 3500 pressure cell represents an average stress value over a larger area. The pressure cell data will be useful to measure the vertical stress on top of the base and subgrade layer.

Installation:

- Prior to installation, the functionality and calibration of each pressure cell was checked by simply placing increments of known dead weight on the cells. The manufacturer provided calibration was used for this experiment.
- The locations of the pressure cell on the test sections was marked with respect to a fixed reference point.
- A cavity and a trench was dug according to the size of the pressure cell. The bottom of the cavity was compacted to create a flat base such that there are no voids between the cell and soil. Small amount of sand was placed between the cell and the base to protect the cell from rocks.
- The pressure cell was leveled by using a level. After leveling, the cavity and trench was backfilled with soil.

- After construction, the location, elevation, and functionality of each pressure cell was confirmed.
- Some invalid pressure measurements have noticed, because of damage during construction.

Tokyo Sokki KML 100 HAS & PML 60. The purpose of embedded strain sensors is to measure the dynamic strain responses at the bottom of the RCC layer in the center of the wheelpath under moving loads.

Installation:

- Prior to installation, the functionality of each strain gauge was checked and manufacturer provided calibration was used for the experiment.
- The locations of the strain gauge on the test sections was marked with respect to a fixed reference point.
- Precautions were taken during construction of RCC layer to minimize disturbance of gauges.
- After construction, the location, elevation and functionality of each strain gauge was confirmed to check the survival.

Time Domain Reflectometer (TDR) CS-616. Moisture content in soils can be important for understanding drainage and soil strength. For this reason, most APT facilities attempt to measure moisture using TDR. TDR is a method of measuring high-frequency electrical signal propagation times, typically in the nanosecond range. TDR technology is applied to soils to indirectly measure the average dielectric properties of the soil system.

Installation:

- Prior to installation, the functionality and calibration of each TDR was checked. The calibration was done by measuring the moisture content of three different soil (A-6) sample of different moisture content (3%, 5%, and 10%). The soil was collected from the PRF site. The calibration results are shown in figure 11 which is different from the manufacturer provided calibration.
- A trench was dug according to the size of the TDR and TDR was horizontally inserted into the subgrade soil. Care was taken to avoid creating any voids between the probes and soil. The trench was backfilled with soil and compacted with care.

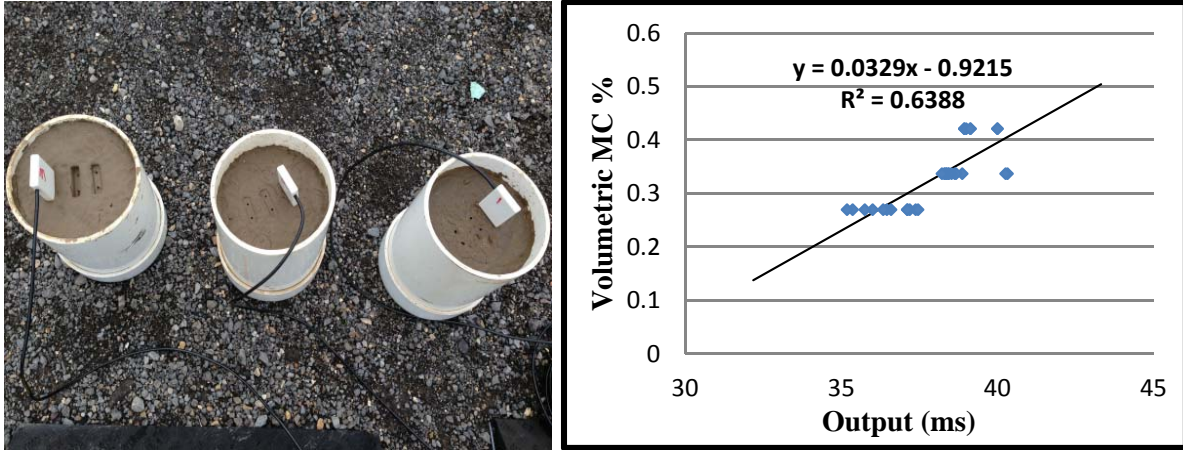


Figure 11
TDR calibration

Temperature Probe. Thermocouples are the most commonly used temperature measuring devices at APT facilities. However, T108 L temperature probe has been used for this experiment to get the temperature variation along the thickness of the RCC slab.

Installation:

- Prior to installation, the functionality of each temperature probe was checked.
- Temperature probe was placed at different depths (2 in. and 4 in. below surface for the 4-in. RCC slab., 2 in., 4 in., and 6 in. below surface for the 6-in. RCC slab).

Joint Deflection Measurement Device (JDMD). JDMD was used to measure joint movement under dynamic load and temperature changes. The JDMD consists of two hermetically sealed GCD-500 LVDTs for measuring the displacement of the slab.

Installation:

- Prior to installation, the functionality of the LVDTs was checked.
- For installation of the JDMDs, a special type of steel frame was used to hold the LVDTs.
- One JDMD was used at the saw cut joints to measure the joint movement of the RCC layer.

Figure 12 shows the various instruments used for this experiment.



(a) Pressure cell



(b) Strain gage



(c) Protecting the wires



(d) JDMD



(e) TDR



(f) Thermo probe

**Figure 12
Instrumentation of RCC test sections**

Data Acquisition Systems. National Instruments (NI) DAQ hardware was utilized to collect data from pressure cell, strain gages, and JDMDs. Campbell Scientific data logger was utilized to collect data from thermo-probe and TDR. Data acquisition and archiving requires appropriate software configured for each experimental setup. For this experiment, data was collected using National Instruments LabVIEW ver. 12 and Campbell Scientific PC400 software. Built in pre-processing signal filtering in the data acquisition hardware and software helped to produce a clean signal. However, electronic noise was encountered while examining the data. A 10-point moving average of data points was used to get clean signals by eliminating the noise. The raw data files were saved into separate folders and subfolders according to the test date, dual tire load, repetition, section number, and data type.

Accelerated Loading Experiment

APT Loading Device

A heavy vehicle load simulation device (ATLaS30) was used for the accelerated loading of RCC test sections in this experiment. As shown in Figure 13, the ATLaS30 device is 65 ft. long, 7 ft. high, and 10 ft. wide, constructed around two parallel steel I-beams. The ATLaS30 wheel assembly models one-half of a single axle and is designed to apply a dual-tire load up to 30,000 lbf by hydraulic cylinders. The ATLaS tire prints under different loads are presented in Figure 14. With a computer-controlled loading system, the weight and movement of traffic is simulated repetitively over a 40-ft long loading area in bi-directional mode at a top speed of 6 mi/hr. By increasing the magnitude of load and running the device for 24 hours a day, it is possible to condense 20 years of loading into a period of only one month. An incremental loading sequence (e.g., 9, 16, 20, 22, and 25 kips) of the ATLaS30 dual tire load is expected to be applied in order to fail each RCC pavement section in fatigue cracking within a reasonable time frame.



Figure 13
The ATLaS30 device

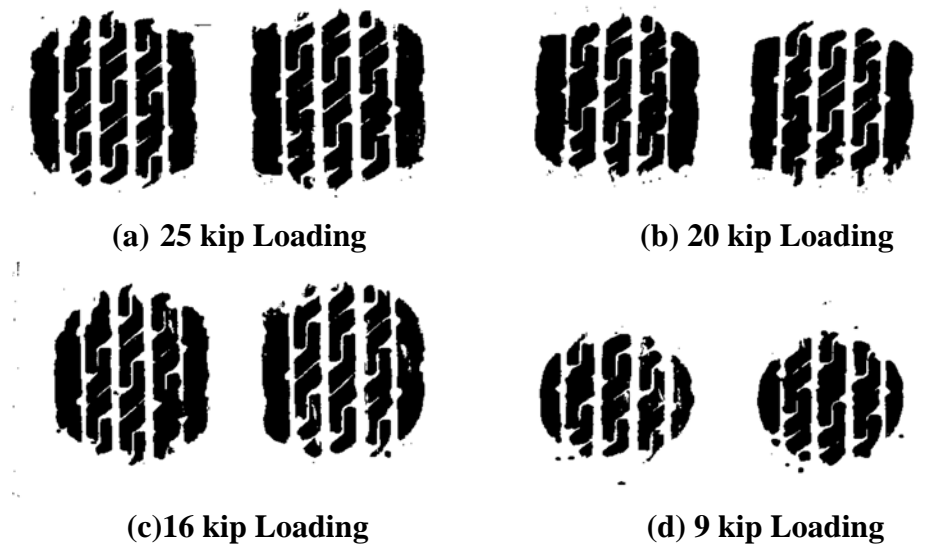


Figure 14

The measured tire prints under different loads

Failure Criteria and Loading History

For this experiment, a test section was considered to have failed when 40% of the trafficked area of a section developed visible cracks (e.g., longitudinal, transverse, and alligator cracks) more than 1 ft/ft².

The accelerated loading test started on Section 4, followed by Section 5, Section 6, Section 3, Section 2, and Section 1 in a time sequence order (Figure 4). Each test section was loaded by an incremental loading sequence of 9, 16, 20, 22, 25, and 27.5 kips. Table 3 provides a list of different dual-tire load magnitudes with the corresponding loading repetitions applied on each RCC sections. Note that, for Sections 1 and 4, due to having a relatively thick RCC slab thickness (i.e., 8 in.), only limited numbers of loading were applied. All other four sections were loaded till pavement failure of cracking.

Table 3
APT loading passes and load magnitudes

| Half Axle Load (kips) | ATLaS30 Dual-Tire Loading Passes | | | | | |
|-----------------------------|----------------------------------|-----------|-----------|-----------|-----------|-----------|
| | Section 1 | Section 2 | Section 3 | Section 4 | Section 5 | Section 6 |
| 9 | ≈ 50,000 | 108,000 | 73,000 | 78,500 | 112,000 | 78,500 |
| 16 | | 265,000 | 73,000 | 78,500 | 404,000 | 392,500 |
| 20 | | 108,000 | 50,000 | 78,500 | 398,000 | 78,500 |
| 22 | | 108,000 | | 78,500 | 108,000 | 78,500 |
| 25 | | 106,000 | | 78,500 | 487,000 | 78,500 |
| 27.5 | | | | | 241,850 | |
| Total Passes | | ≈ 50,000 | 695,000 | 196,000 | 392,500 | 1,750,850 |
| Estimated MESALs | - | 19.4 | 2.7 | - | 87.4 | 19.2 |

In this study, the predicted ESAL numbers were computed using an equivalent axle load factor (EALF) multiply by the corresponding number of load repetitions under a certain ATLaS30 axle load. The EALFs for different ATLaS30 axle loads were estimated based on the AASHTO's rigid pavement equations as follows [22]:

$$\log(EALF) = 4.62 \log(18+1) - 4.62 \log(L_x + L_2) + 3.28 \log L_2 + \frac{G_t}{\beta_x} - \frac{G_t}{\beta_{18}} \quad (4)$$

$$G_t = \log \left(\frac{4.5 - p_t}{4.5 - 1.5} \right) \quad (5)$$

$$\beta_x = 1.00 + \frac{3.63(L_x + L_2)^{5.20}}{(D+1)^{8.46} L_2^{3.52}} \quad (6)$$

where, L_x is the load in kip on different axles;
 L_2 is the axle code, 1 for single axle, 2 for tandem axles, and 3 for tridem axles;
 p_t is the terminal serviceability, which indicates the pavement conditions to be considered as failures;
 D is the slab thickness in inches.

Field Measurements and Non-Destructive Testing

During and after Construction. The Falling Weight Deflectometer (FWD) deflection test and density measurements were performed on the completed surfaces of all

base and subgrade layers during the construction. Shortly after the construction, a suite of in-situ tests were performed on the finished RCC surfaces, including sand patching, Dynamic Friction Tester (DFT), walking profiler, and FWD. A Dynatest 8002 FWD was used in this experiment with nine sensors spaced at 0 in., 8 in., 12 in., 18 in., 24 in., 36 in., 48 in., 60 in., and 72 in. from the center of the load plate.

Figure 15 shows a picture of each in-situ tests used. Specifically, the sand patch test was used to determine the average macrotexture depth (MTD) of the finished RCC surfaces; whereas, the DFT test was to measure the corresponding pavement surface friction. In addition, an ARRB Walking Profiler G2 was used to measure the centerline profilers of the finished RCC surfaces. A software named “ProVAL” was used to convert a measured longitudinal profile into the International Roughness Index (IRI) number for each RCC pavement section tested [23].

During the ATLaS Loading. Instrumentation data and surface profiles were collected on a weekly base on the tested section during the loading experiment. The instrumentation data include the vertical stresses, and longitudinal and transverse strains at the bottom of RCC layers as well as RCC temperatures and subgrade moistures. In addition, surface cracking maps were prepared periodically at different load repetitions.



(a) Sand Patch Test (b) Dynamic Friction Tester (c) Walking Profiler (d) FWD Testing

Figure 15

In-Situ and non-destructive testing

Data Analysis Techniques

The data analysis of this study include the processing of NDT deflection data, evaluation of instrumentation results, modeling RCC pavement structure and fatigue analysis, and prediction of RCC pavement cracking performance. The following analysis procedures and software are used in this study.

ELMOD 6 Method. ELMOD is an acronym for Evaluation of Layer Moduli and Overlay Design [24]. It includes a FWD backcalculation module based on the Odemark-Boussinesq method. The ELMOD 6 program was used to backcalculate the layer moduli of RCC sections in this study.

KENPAVE. KENPAVE includes KENLAYER and KENSLAB. KENSLAB is a finite element (FE) computer program that can be used to predict the load-induced stresses, strains, and deflections in rigid pavements.

ISLAB2000. ISLAB2000 is a 2.5-dimensional FE-program, specially constructed for calculating stresses and strains in concrete slabs very fast, can be used to calculate the critical tensile stresses of different pavement structure. These programs are simple in a way that a number of adjacent slabs and pavement shoulders can be modeled with specific interaction properties. One of the most helpful advantages of ISLAB2000 is the possibility to calculate both temperature and traffic stresses at the same time. Nonlinear temperature gradients are also possible to model in ISLAB2000.

StreetPave. StreetPave is a pavement design tool geared primarily to streets and roads. It is based on the PCA's pavement thickness design methodology and used for both existing and new pavement design.

DISCUSSION OF RESULTS

The results were obtained from both laboratory and APT measurements, including the mixture strengths, moisture-density curves, NDT, instrumentation data, surface crack mapping, and forensic trenches on failed RCC test sections. In addition, the fatigue performance of thin RCC pavements was analyzed in details, which has led to the development of fatigue equations for thin RCC pavement structures. Subsequently, a thickness design procedure was proposed. Finally, an economic analysis was performed to assess the cost benefits and potential use of thin RCC surfaced pavement as a design option for the DOTD's low-volume roads where heavy truck trafficking is often encountered.

Results from Laboratory Tests

RCC Mix Design

Moisture verse Density Curves. Figures 16 to 19 show the moisture density characteristics for the 350, 400, 450, and 500 pcy cementitious contents, respectively, during the job mixture design of RCC. The results show that the maximum density tends to increase as the cement content increases. This is due to the larger amount of fine material that leads to better particle packing resulting in an increased density. The optimum moisture content for all mixtures ranges from 6.5 to about 7%. These mixtures contained about 53% coarse and 47% fine aggregate by weight. Note that the mixtures were harsh and difficult to work with at this ratio. The ratio was then later revised to a 43% coarse and a 57% fine aggregate by weight ratio to provide a denser pavement structure and a better overall surface finish.

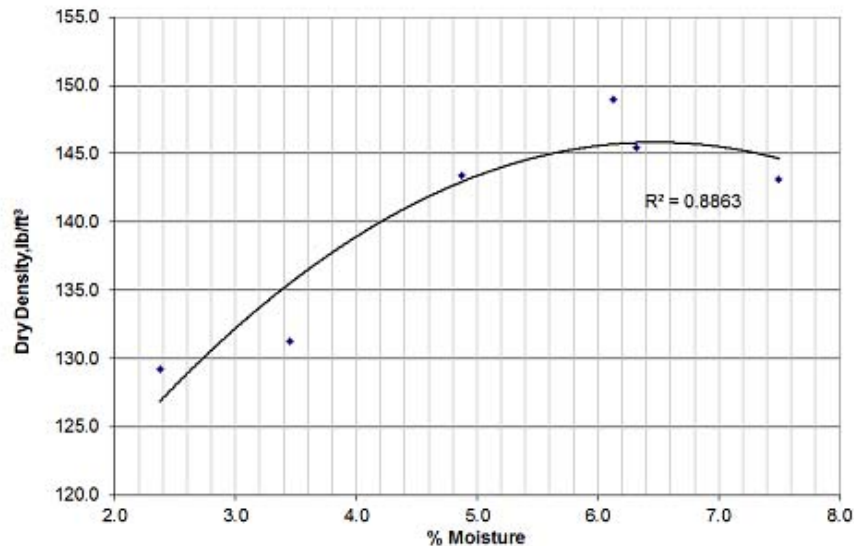


Figure 16

Moisture density relationship for 350 pcy cement content mixture

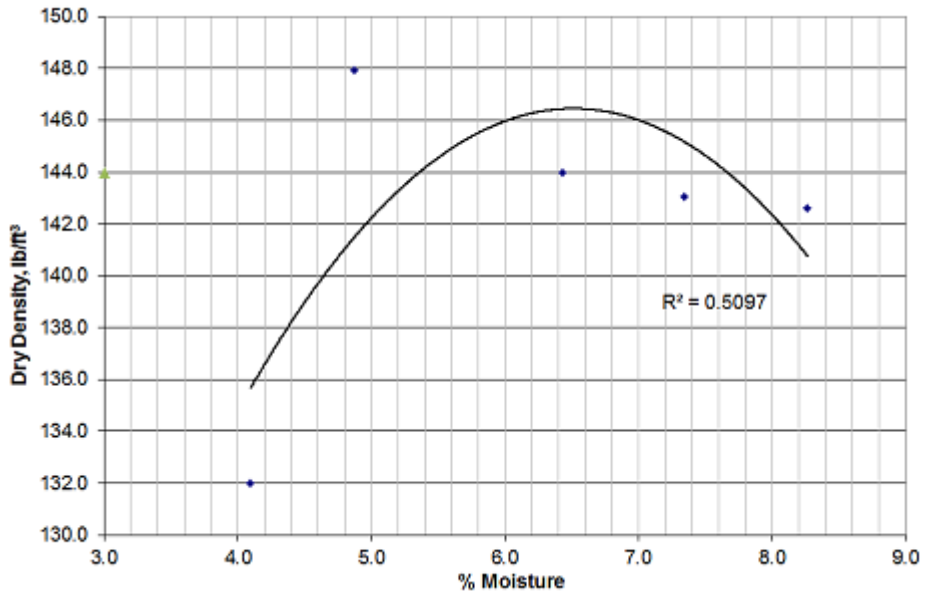


Figure 17
Moisture density relationship for 400 pcy cement content mixture

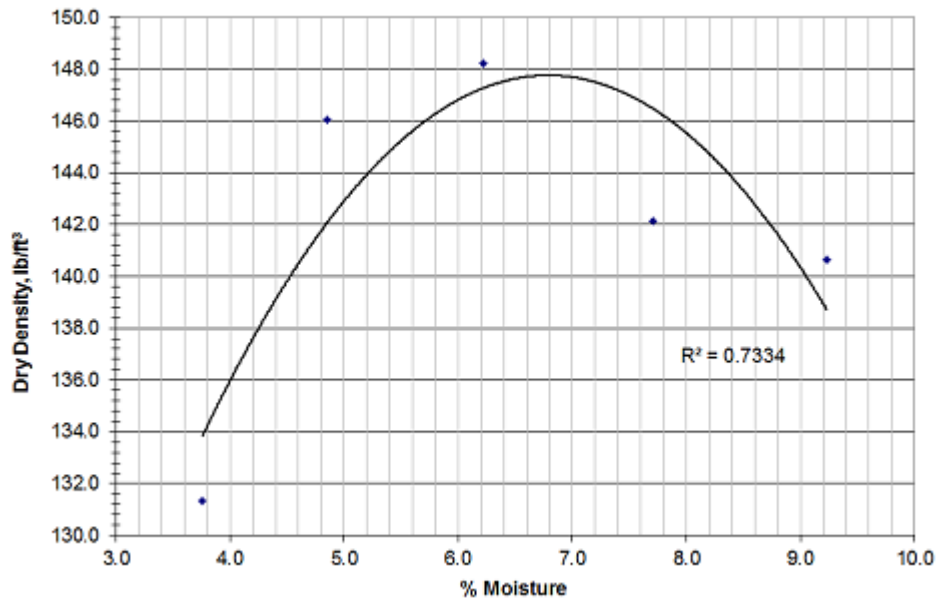


Figure 18
Moisture density relationship for 450 pcy cement content mixture

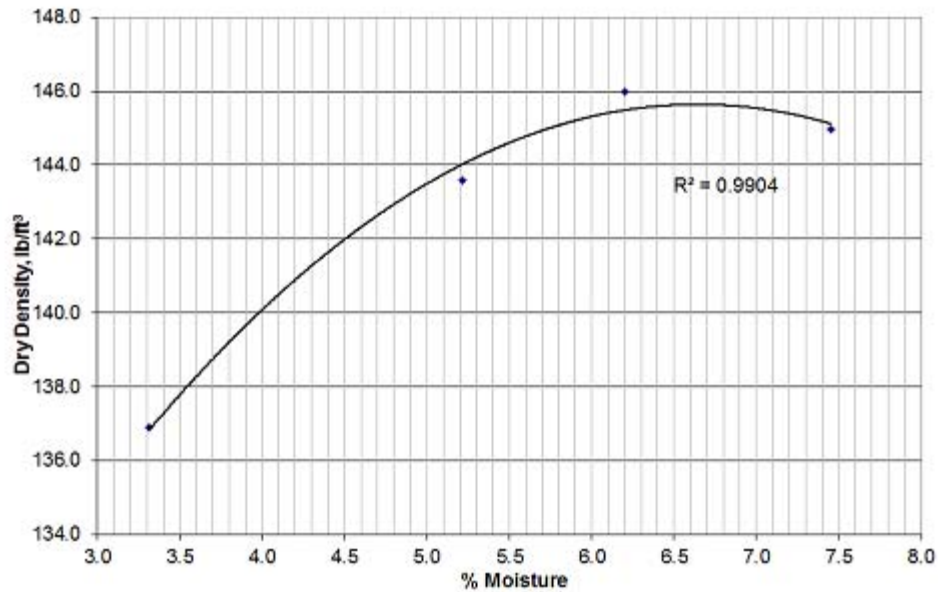


Figure 19
Moisture density relationship for 500 pcy cement content mixture

Compressive Strengths. Figure 20 shows the compressive strength results for all lab-produced mixtures tested. Note that the compressive strength increased as the cement content increased as expected. The target strength for the mixture was set at 4000 psi at 28 days of age. The compressive strength results were as expected with the strengths increasing with an increase in cement content. The mixture designated as “450 new gradation” was measured at the request of the contractor performing the mixing of the RCC as it was a slightly better fit to the 0.45 gradation limits. Note that it outperformed the original gradation and almost equaled the 500 pcy mixture.

The results show that all mixtures meet the required 4000 psi as early as 7 days of age. Much debate occurred as to which mixture was the optimum, or minimum, cement content required for the construction of the test lanes. The research team determined the 450 pcy mixture to be acceptable as it provided the density characteristics desired and a sufficient factor of safety for strength considerations as the lanes were constructed.

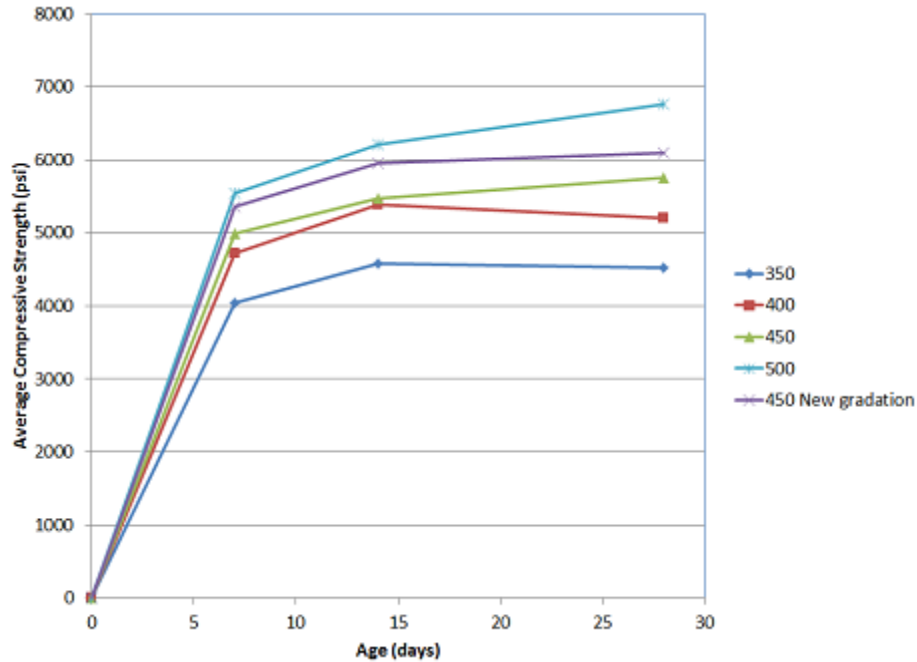


Figure 20
Compressive strength results for all mixtures

RCC Used in Test Lanes

Compressive Strengths. Figure 21 shows the average compressive strength results for samples produced for Lane 1 and 2 as well as cored specimens from Lane 1 and 2. Note that the cored specimens are the 55-day specimens. The results are as expected and matched laboratory cured specimens well. The overall compressive strength at 28 days was found exceeding 5,000 psi. Note that the 1-day compressive strength results were relatively low when compared to normal RCC. This is due to the overnight low temperature after construction was recorded at 37 degrees Fahrenheit. The cored specimens were slightly less than the field produced samples due to differences in density. Field produced specimens were slightly denser (i.e., greater than 98% density) compared to the paver consolidated samples.

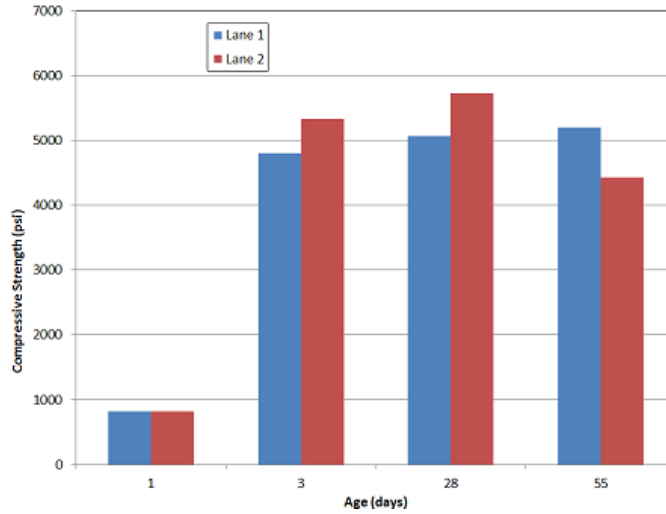


Figure 21

Average compressive strength results for samples produced for Lane 1 and 2

Flexural strength. An average flexural strength of the saw-cut RCC beam samples was 661 psi. It should be pointed out that all the cylindrical samples and field cores achieved the adequate strength requirements for this experiment. However, the overall compressive strength for Lane 1 (including Sections 1-3) was found approximately 10% lower than that of Lane 2 (including Sections 4-6). This could be due to a high paving/construction speed used on Lane 1, which subsequently was reduced when paving on Lane 2. Higher paving speed could have resulted in a lower density and strength for Lane 1 than those for Lane 2.

Results from RCC APT Test Sections

Surface Characteristics and In-Situ Density

Figure 22 shows the surface characteristics of the constructed sections. The DFT, sand patching, and walking profile test results are presented in Table 4.

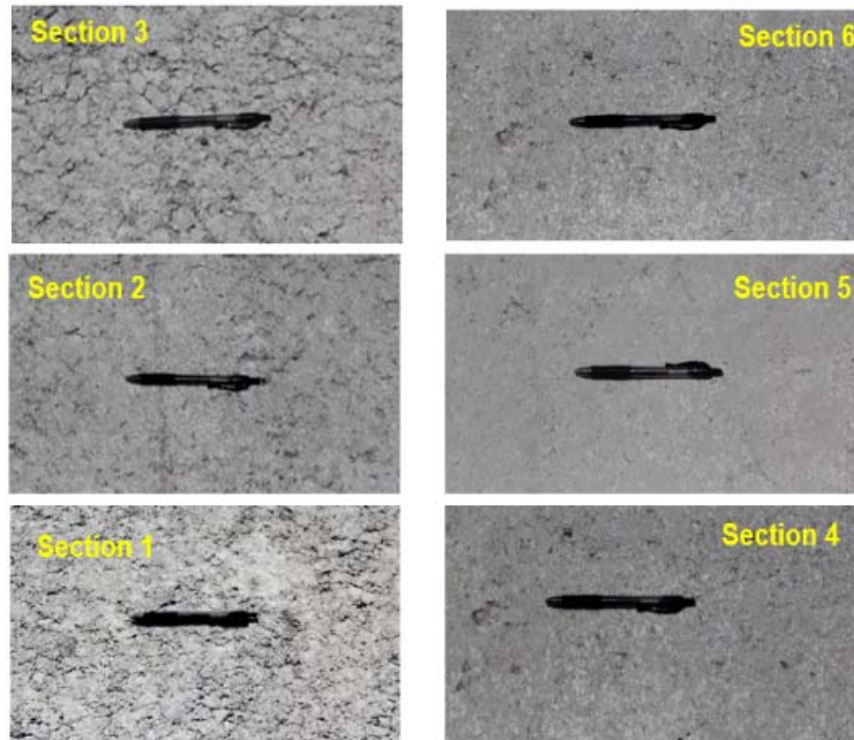


Figure 22
Surface texture of the constructed test sections

The DFT20 value shown in the table represents the DFT measured friction number at 20 km/h, which is often used as an indicator for surface micro-texture of a pavement [25]. In general, the measured DFT20 values of RCC test sections ranged from 0.22 to 0.42, which are in a similar range as those measured on the top of different asphalt mixtures. On the other hand, the measured MTD values varied from 0.36 to 0.99 that are also similar to those of asphalt concrete surfaces [25]. Overall, it is felt that RCC pavement surfaces should have a similar surface friction characteristic as asphalt concrete surfaces, in terms of both micro- and macro- textures.

Table 4
Sand patching and DFT test results

| Section | DFT20 | MTD (mm) | IRI (in/mile) |
|----------------|--------------|-----------------|----------------------|
| Section 1 | 0.3 | 0.99 | 360 |
| Section 2 | 0.4 | 0.72 | 470 |
| Section 3 | 0.22 | 0.89 | 623 |
| Section 4 | 0.3 | 0.36 | 190 |
| Section 5 | 0.42 | 0.39 | 122 |
| Section 6 | 0.28 | 0.43 | 168 |

As shown in Figure 22 and Table 4, the surface texture for Sections 1-3 is significantly more rough than the surface texture for Sections 4-6, in terms of IRI. This is most likely due to paver speed as Lane 1 was constructed in roughly 2/3 of the time as Lane 2 resulting in a rougher pavement surface. The IRI is also increased due to the frequent change in pavement thickness as the lanes were paved. Each section is roughly 70 ft. in length leading to frequent pavement thickness transitions. It is known that using diamond grinding or a thin asphalt overlay on top of RCC would overcome the rough surface issue. However, based upon the field results, IRI values in the 100-120 in. per mile range (similar as the results from Section 5) and compressive strengths exceeding 5,000 psi would be expected in a full scale roadway construction effort of a thin RCC-surfaced pavement.

Field nuclear density results are shown in Table 5. Note that about half of the sections did not meet the minimum density of 98% wet density as specified in the construction requirements. The low density results were noted and all sections were measured above 96% density.

Table 5
Nuclear density test results for RCC test sections

| Section Number | Density (%) |
|-----------------------|--------------------|
| 1 | 96.8 |
| 2 | 97.1 |
| 3 | 97.9 |
| 4 | 98.9 |
| 5 | 98.5 |
| 6 | 98.1 |

A one point-field Proctor specimen was produced during RCC lane construction to verify that the mixture was meeting or exceeding the laboratory design. Figure 23 shows the results of the one-point Proctor specimen. Note that the measured wet and dry densities fell on the curve, even if the mixture was very dry of optimum.

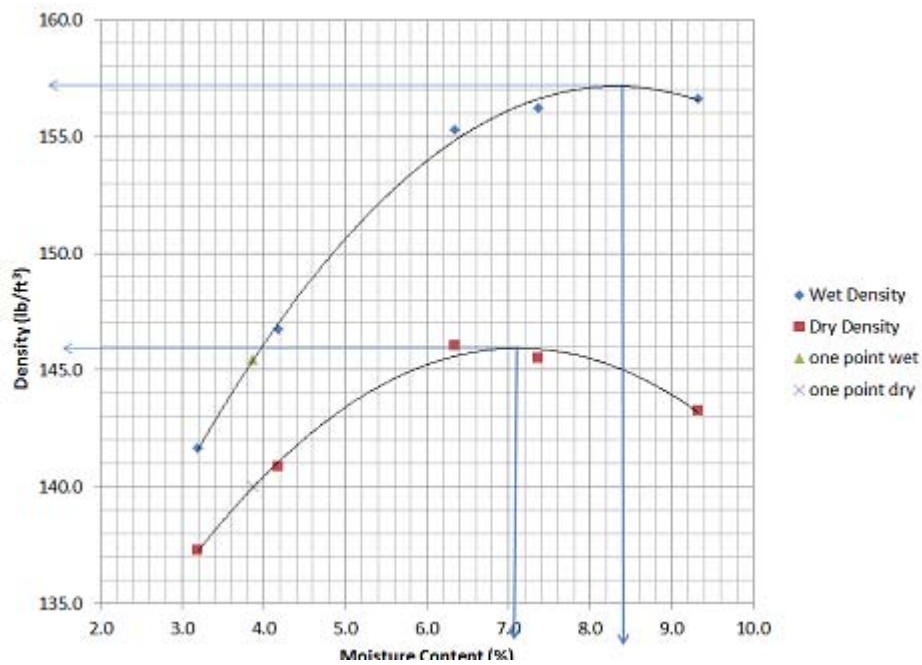


Figure 23
One-point Proctor specimen

Slab Thicknesses and Backcalculated Layer Moduli

Three cores were taken and measured from each constructed RCC test section and averaged for the section thickness. The thickness results for each section are shown in Table 6.

Table 6
Thickness variation of RCC sections

| Section Number | Thickness (in.) |
|-----------------------|------------------------|
| 1 | 9.65 |
| 2 | 6.05 |
| 3 | 4.90 |
| 4 | 8.01 |
| 5 | 6.36 |
| 6 | 4.10 |

The core thickness results show that the sections were built over the designed thickness. This is due to a sloping subgrade with a level pavement surface. The IRI results for Sections 1-3, in Lane 1, were significantly higher than the IRI results for Sections 4-6. This is most likely due to paver speed as Lane 1 was constructed in roughly 2/3 of the time as Lane 2 resulting in a rougher pavement surface. The IRI is also increased due to the frequent change in pavement thickness as the lanes were paved. Each section is roughly 70 ft. in length leading to frequent pavement thickness transitions. The authors believe that in an actual construction project, IRI values would be equal to or lower than the results from Section 5.

The FWD deflections measured on the finished RCC surfaces were used in the backcalculation of layer moduli for each RCC sections constructed. The ELMOD 6 backclaulcation software package was used and the results are presented in Figure 24 [24].

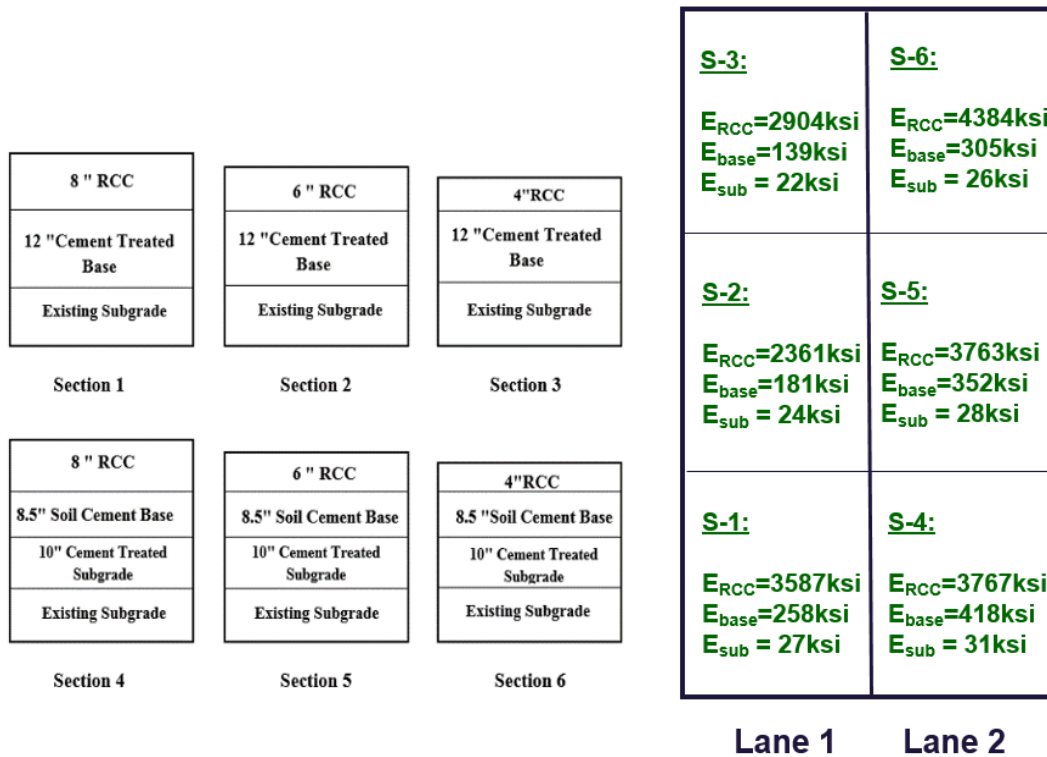


Figure 24
FWD backcalculated moduli of RCC test sections

As expected, the backcaluated moduli of RCC layers in Sections 1-3 are generally lower than those in Sections 4-6, which is consistent with the compressive strength test results obtained in the laboratory. The soil cement layers with 8% of cement content are stiffer in terms of the backcalculated moduli than the cement treated soil layers of 6% cement content. The backcalculated subgrade moduli are also found higher for those sections on Lane 2 due to the 10-in. cement-treated subgrade (Figure 24). Note that the FWD backcalculated subgrade moduli are ranged from 22 to 31 ksi, significantly higher than those commonly-used design subgrade values. According to the 1993 AASHTO pavement design guide, when using FWD backcalculated moduli in pavement design and analysis, a coefficient of 0.33 is needed [22].

Typical Instrumentation Responses

Typical responses of pressure cell and strain gages under ATLaS30's dual tire loads are illustrated in Figure 25. In general, all of those responses are as expected. For example, under the bidirectional dual tire loading, when the wheel is approaching from right to left, the longitudinal strain first shows compression, then tension, and finally compression; and when the wheel is approaching from left to right, it shows tension, then compression, and finally tension again. On the other hand, the transverse strain gage only shows pure tension under

the dual tire loading in both directions, Figure 25. A small difference existed between the two peaks in a bi-directional loading could be due to a slight longitudinal slope of RCC test sections built for the drainage purpose.

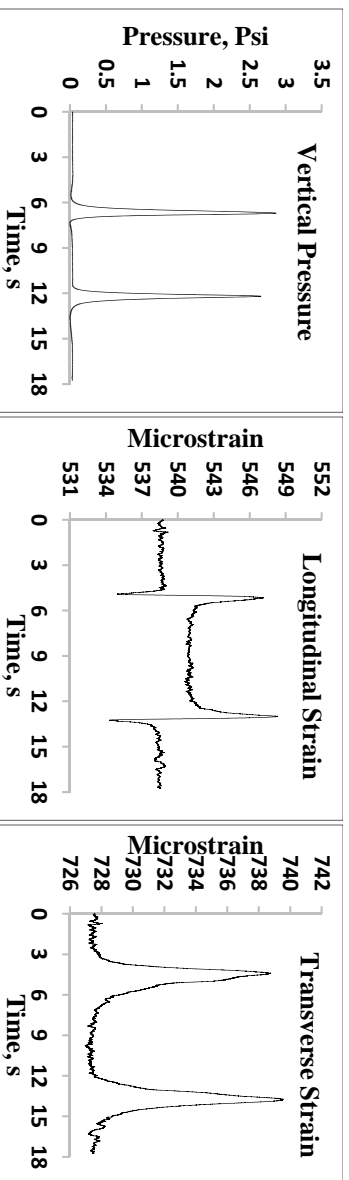
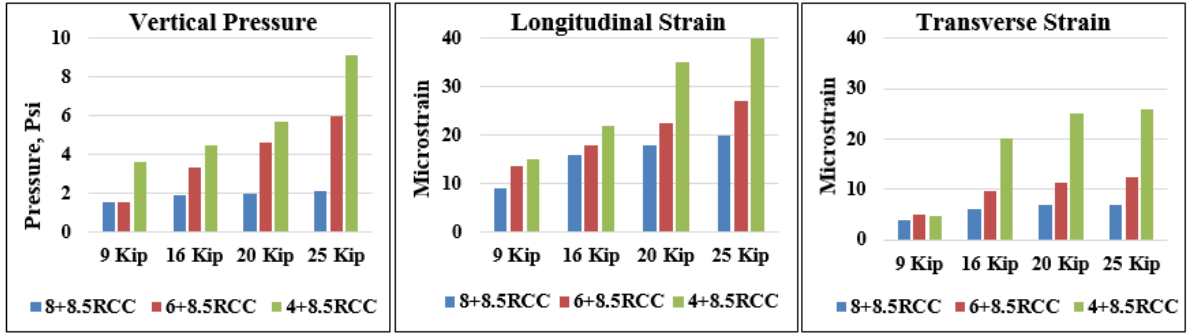
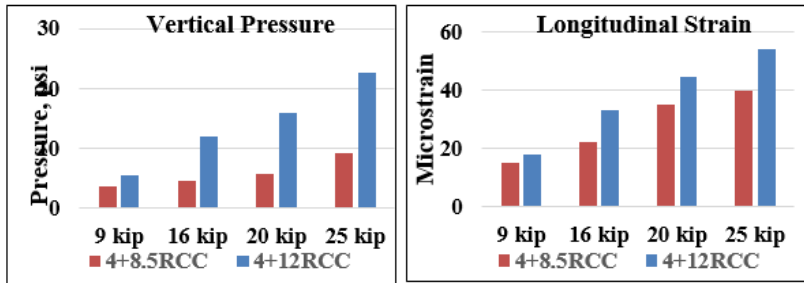


Figure 25
Typical Instrumentation response under ATLAS 30 loading

Figure 26 presents the comparison of typical stresses and strains measured at the bottom of RCC slabs under different load magnitudes for the four RCC sections evaluated. As expected, Figure 26 (a) shows that the measured stresses and strains are all increased with the increasing of load magnitude and decreased with the increase of RCC thickness. When comparing the two 4-in. RCC sections with different base and subgrade layers, Figure 26 (b) indicates that the increasing of the RCC underneath support decreases the load-induced responses, thus, the Section 6 (4+8.5RCC) would be expected to have a better performance (in term of load carrying capacity) than Section 3 (4+12RCC).



(a)



(b)

Figure 26

Comparison of load-induced pavement responses (a) RCC thickness, (b) different bases

Figure 27 shows the typical pavement temperature and subgrade moisture variation throughout the day and temperature variation along the depth of the RCC layer. This data will be further used to analyze the environmental effects and to predict the performance of RCC pavements.

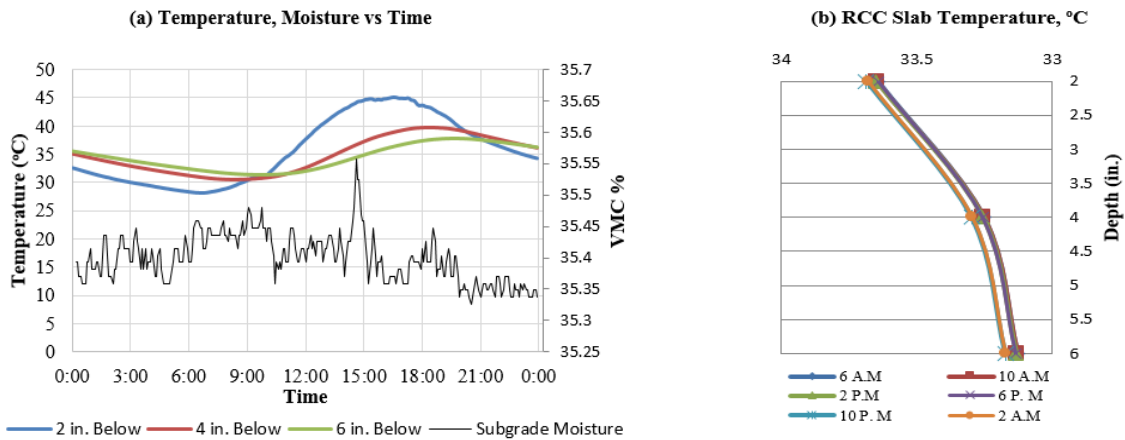


Figure 27

Typical temperature and moisture responses

Performance of RCC APT Sections

At the end of the APT experiment, four sections (Sections 2, 3, 5, and 6) were continuously loaded and found to have reached their respective pavement service lives, as evidenced by the extensive surface cracks and significant surface roughness shown in Figure 28. The two 8-in. RCC Sections of 1 and 4, however, were not loaded to failure due to a concern of possibly extremely-long loading time.



Figure 28
RCC pavement condition at the end of testing

As seen in Table 3 in the Methodology, the estimated pavement lives in terms of total predicted ESALs for the four failed Sections of 2, 3, 5, and 6 were 19.4, 2.7, 87.4, and 19.2 million, respectively. It is important to note here that the predicted pavement lives only represents the RCC pavements under the APT loading condition of this study, in which a dual-tire ATLaS wheel load has been applied in the center of each RCC section lanes. When performing fatigue analysis in an RCC pavement thickness design, the critical tensile stress at bottom of RCC slabs must be determined under a critical loading point (e.g., at the corner or the edge of RCC slabs) using a complete single axle load configuration.

Generally, the estimated pavement lives in Table 3 seemed to match well with the individual pavement structure strengths, that is, a thicker RCC and a strong base provides longer pavement lives. It also showed that Section 2 with a 6-in. RCC over a weaker cement treated base may have a similar pavement life as Section 6 of a 4-in. RCC over a strong soil cement base. Section 3 is the weakest pavement structure (a 4-in. RCC over a 12-in. cement treated base) in this study, in which only 2.7 million ESALs were estimated. However, as listed in Table 3, even this section has endured a large number of heavy axle load (e.g., 50,000

repetitions of 20-kips of ATLaS 30's half-axle load is equivalent to 50,000 repetitions of 40-kips of single axle load). Overall, the APT loading results have indicated that all thin RCC test sections tested have high load carrying capacity under typical southern Louisiana pavement condition. The more substantial foundation used in Sections 5 and 6 generally provided additional structural capacity that may be equivalent to a 2 in. thickness of RCC as compared the less substantial foundation used in Sections 2 and 3.

Post-Mortem Trenches

A post mortem evaluation on the four cracking-failed RCC pavement sections was performed at the end of APT testing. The post mortem trench results provide the following observations:

- The majority of longitudinal cracks under the wheel path are bottom-up cracking, as shown in Figure 29 (a) and (b). In addition, all sections showed voids underneath the RCC layer caused by the loss of material possibly due to erosion and pumping [Figure 29 (c) and (d)].

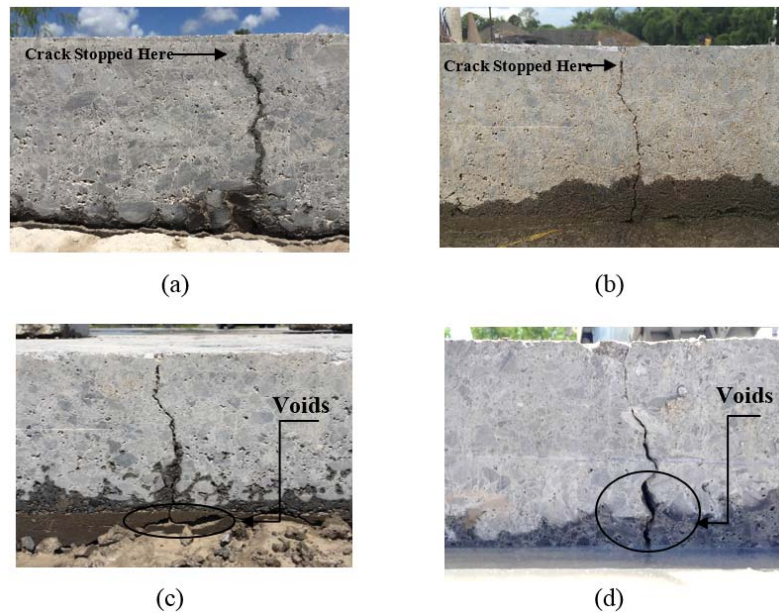


Figure 29

Bottom-up longitudinal cracking and voids under the wheel path.

- However, top-down cracks were detected at a few locations, especially outside the wheel path (Figure 30 (a) and (b)).

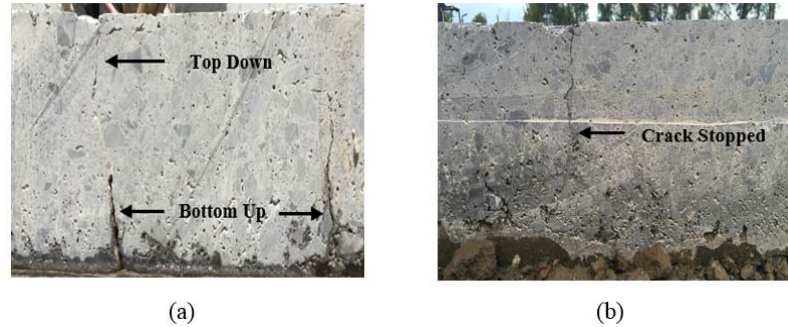


Figure 30

Top-down longitudinal cracks within and outside the wheel path.

- The post mortem results also revealed that the saw cutting joints at severely damaged locations cracked through along the slab thickness (Figure 31).

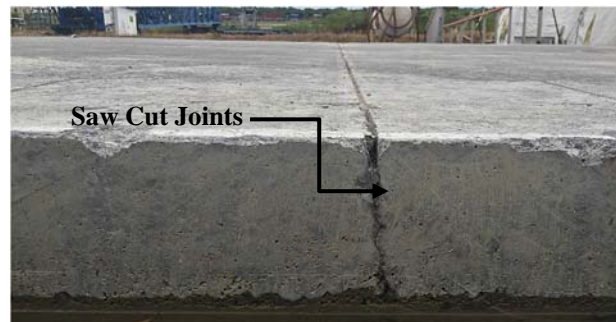


Figure 31

Cracks at the saw-cutting joint

Prediction of Field Tensile Stress and FEA

A preliminary fatigue analysis of RCC test sections was conducted based on the field instrumentation responses. First, the field instrumentation responses were validated using the finite element (FE) program, KENSLAB [22]. As shown in Figure 32, each RCC test section was modelled as a three-layer system-RCC and Base layer over solid foundation in KENSLAB. First, based on the FWD backcalculation results a modulus value of 4,000Ksi was chosen for all RCC layers to represent an overall average modulus of this material in a field condition. Second, a set of modulus values of 250 to 800Ksi and 100 to 600Ksi was selected to represent the 8.5 in. soil cement base layer and 12 in. cement treated base layer, respectively. The interaction between the RCC slab and the base layer was considered to be as fully bonded. Finally, based on the results of elastic analysis using KENSLAB, a modulus value of 15Ksi and 20Ksi were selected to model the solid foundation layer to represent the

existing subgrade condition and 10-in. cement treated subgrade, respectively. Different modulus values for the base layer were considered in the model to represent the in-situ characteristics of the subgrade and base layer in the field followed by the FWD responses. As presented in Table 7, when those selected modulus values were applied in the elastic analysis under a FWD load, the predicted surface deflections matched fairly well with those measured deflections under different FWD loads, except the FWD load of 9000-lbf.

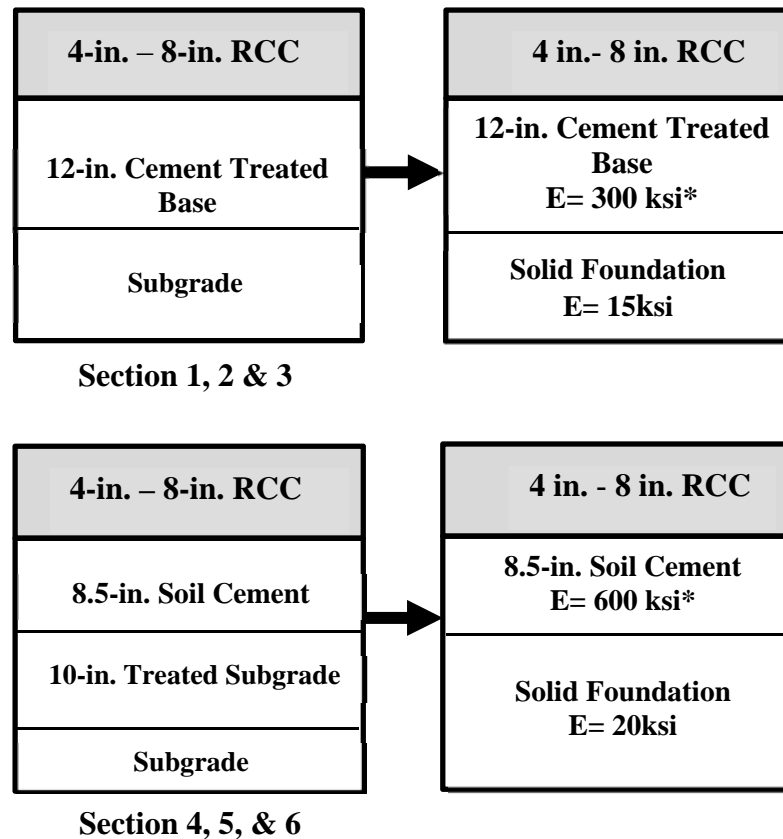


Figure 32
RCC pavement structures used in finite element analysis

The field critical tensile stress at the bottom of RCC slabs was estimated from the instrumentation responses. First, it was considered that the pressure cell, longitudinal strain gage, and transverse strain gage are at the same location giving the pavement responses (vertical stress, longitudinal strain, and transverse strain) at a single point. Second, considering the Hook's law and assuming RCC layer as a homogeneous elastic layer with a modulus value of 4000Ksi with a poisson's ratio of 0.15, the field critical tensile stress was estimated under different ATLaS dual tire loads by solving the simultaneous equations. The field estimated tensile stress at the bottom of RCC layer matched fairly well with the

predicted critical tensile stress from KENSLAB model under different loading condition, Table 7. The predicted and estimated tensile stress for all the sections were found to be in good agreement corresponding to the pavement structure, while the estimated values were smaller than the predicted values. This could be due to the dynamic loading condition in the field and other environmental effects. A more realistic FE model will be developed in future to better predict the pavement responses.

Table 7
Field measured and predicted responses of RCC test sections

| Sections | FWD Load | Measured Deflection D0 (in.) | Predicted Deflection (in.) | Estimated Field Tensile Stress (psi) | Predicted Tensile Stress (psi) |
|-----------------|----------|------------------------------|----------------------------|--------------------------------------|--------------------------------|
| 6+8.5RCC | 9 kip | 0.00052 | 0.0052 | 59.82 | 64.50 |
| | 16 kip | 0.00810 | 0.00880 | 79.98 | 97.23 |
| | 20 kip | 0.01020 | 0.01101 | 100.06 | 121.21 |
| | 25 kip | 0.01288 | 0.01371 | 120.14 | 143.80 |
| 4+8.5RCC | 9 kip | 0.00071 | 0.00664 | 64.96 | 90.11 |
| | 16 kip | 0.01121 | 0.01154 | 103.10 | 129.84 |
| | 20 kip | 0.01410 | 0.01444 | 159.57 | 164.43 |
| | 25 kip | 0.01773 | 0.01792 | 181.25 | 193.46 |
| 4+12RCC | 9 kip | 0.00086 | 0.00801 | 77.52 | 107.76 |
| | 16 kip | 0.01340 | 0.01411 | 141.41 | 158.93 |
| | 20 kip | 0.01680 | 0.01767 | 190.62 | 198.18 |
| | 25 kip | 0.02117 | 0.02196 | 230.49 | 233.83 |
| 6+12RCC | 9 kip | 0.00582 | 0.00607 | 49.1 | 71.610 |
| | 16 kip | 0.00752 | 0.01065 | 67.6 | 108.253 |
| | 20 kip | 0.00952 | 0.01332 | 94.6 | 135.022 |
| | 25 kip | 0.0164 | 0.01659 | 117.5 | 160.592 |

Analysis of Cracking Potentials of Thin RCC Pavements

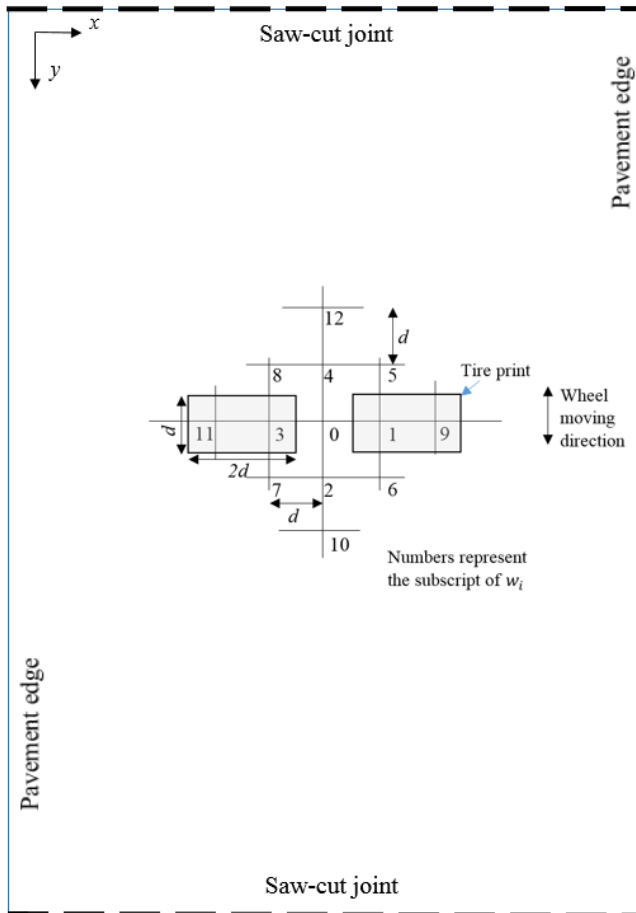
Traditionally, the critical cracking failure for a rigid pavement would be the cracks initiated at the bottom of the rigid layer due to repeated fatigue loading. However, field observations of cores and trench sections from in-service pavements have shown that premature failures may develop from the surface and propagate their way down, such as top-down cracking [26-27]. Recently, it was found that the crack could also initiate from the near-surface of rigid pavements.

In this study, a finite difference model was developed to predict the load-induced critical tensile flexural stresses and subsequently investigate the cracking performance of thin RCC-surface pavements. For an elastic thin slab on a Winker foundation (liquid foundation), the differential equation of the slab can be written as:

$$\frac{\partial^4 w}{\partial x^4} + 2 \frac{\partial^4 w}{\partial x^2 \partial y^2} + \frac{\partial^4 w}{\partial y^4} + \frac{k}{D} w = \frac{q}{D} \quad (7)$$

where x and y are the horizontal direction and vertical direction, respectively; w is the slab deflection; k is the subgrade reaction modulus; D is the slab stiffness, $D = \frac{Eh^3}{12(1-\mu^2)}$, in which E is the elastic modulus of the slab, h is the slab thickness, μ is slab Poisson's ratio; and q is the applied pressure.

Figure 33 presents a schematic representation of the developed finite difference model including the pavement geometry, relative node locations, and tire print as well as the derived finite difference step equation and equations for calculating of the critical tensile flexural stresses at bottom of RCC slab in x and y directions under a load.



Rewrite Equation (1) in a finite difference form

$$\left(20 + \frac{k d^4}{D}\right) w_0 - 8(w_1 + w_2 + w_3 + w_4) + 2(w_5 + w_6 + w_7 + w_8) + (w_9 + w_{10} + w_{11} + w_{12}) = \frac{q_0 d^4}{D} \quad (2)$$

$$\sigma_x = \frac{Eh}{(1-\mu^2)d^2} [(2 + 2\mu)w_0 - (w_1 + w_3) - \mu(w_2 + w_4)] \quad (3)$$

$$\sigma_y = \frac{Eh}{(1-\mu^2)d^2} [(2 + 2\mu)w_0 - \mu(w_1 + w_3) - (w_2 + w_4)] \quad (4)$$

where d = the step length of the finite difference operation

w_i = slab deflection at node i

σ_x = the flexural tensile stress in the x direction

σ_y = the flexural tensile stress in the y direction

Figure 33

Relative locations of nodes and tire print in the finite difference model

In the analysis, the tire print of a 9-kip ATLaS load with tire pressure of 130 psi was modeled in a dimension of 4.5 in. by 9 in. ($d \times 2d$) for the convenience of the finite difference analysis, as shown in Figure 33. Since the aim is to investigate the cracking potential in a thin RCC slab, the simplification is deemed reasonable and will not influence the prediction results. In the analysis, the following representative parameters were used: 13-ft slab width, 6-in. slab thickness, 3000 ksi slab modulus, and 500 pci subgrade reaction modulus.

- Before the joint cracked, a 20-ft long RCC section with the representative parameters was modeled with a joint in the middle length. Considering a load moving towards a saw cut joint, Figure 34 shows the predicted critical (maximum), bottom-up flexural stresses at bottom of the joint in both x and y directions. As shown in Figure 34, the maximum flexural stress is σ_y , which is the stress that potentially causes a transverse cracking. This result indicates that, under the repetitive wheel loading, fatigue cracks could be first generated at the bottom of a saw-cut joint and eventually reflected to the joint surface (i.e., transverse cracking). In other words, a saw-cut joint, due to its thinner slab thickness, is possibly the weakest location on a thin RCC pavement where the fatigue cracking damage may be initiated.

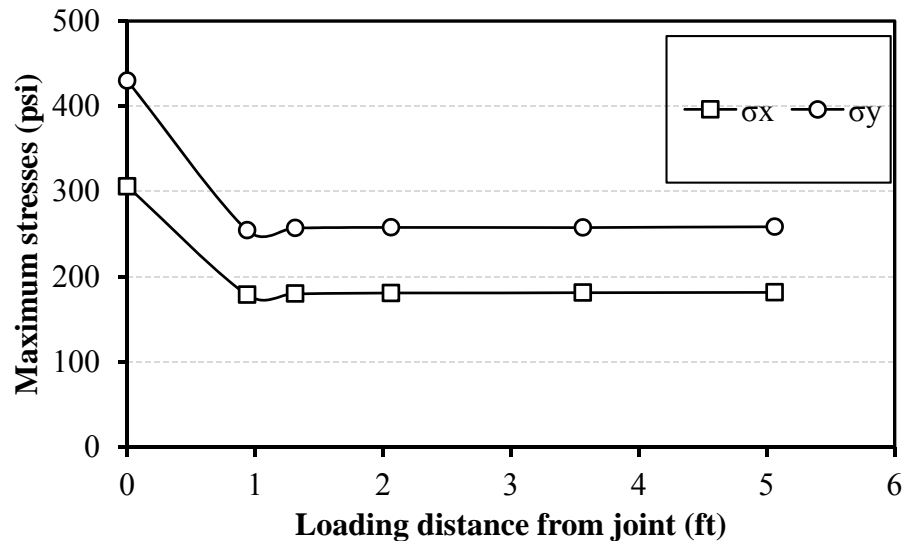


Figure 34

Maximum flexural stresses versus the distance of loading from joint

- After the crack through the saw cut joint, the RCC slab can be considered as a free edge slab on the Winker foundation. To detect the crack potential of a thin RCC slab, load was applied at the center and the edge respectively. Figure 35 shows the maximum flexural stress with the increase of the slab length for a slab with a width of

13 ft. As shown in the figure, the edge loading causes a much higher flexural stress σ_x than σ_y . In addition, the flexural stress σ_x caused by the edge loading is not sensitive to the slab length. When the load is applied at the center, the flexural stress σ_y at the center increases while σ_x decreases with the increase of the slab length. After the slab length is higher than 7.2 ft., the flexural stresses at the center become stable and σ_y is higher than σ_x . In summary, with the load moving from the edge to the center, the maximum flexural strength is σ_x at the edge. The stress will potentially cause a bottom-up longitudinal cracking within the wheel path at the edge of the slab.

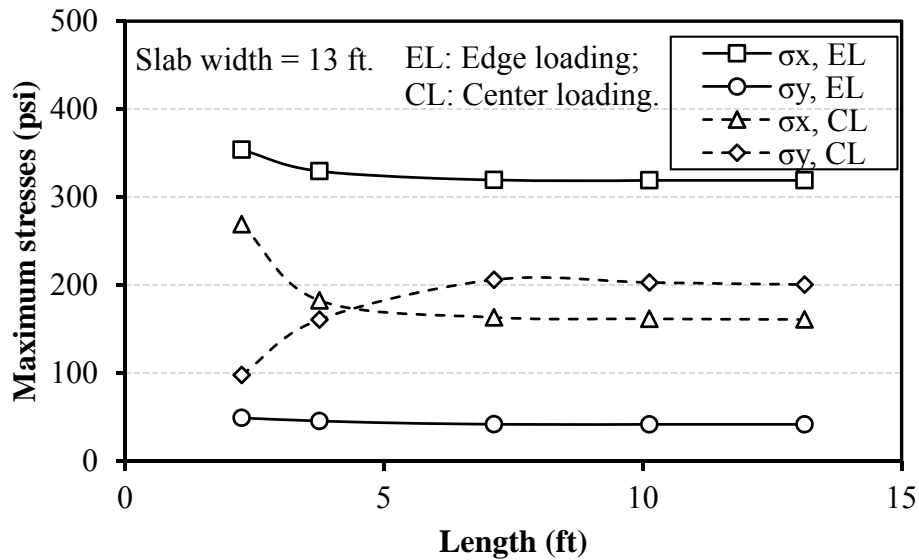


Figure 35

Maximum flexural stresses versus the length of the slab

- After the joint cracked through and the longitudinal crack occurred, pumping under the cyclic loading became a serious problem after rain events. Due to the loss of fine particles, a separation zone generated beneath the slab and, consequently, the cracking potential of the pavement was increased. Figure 36 shows the flexural stresses versus the length of the separation zone. As shown in the figure, for the edge load, the flexural stresses increase with the expansion of the separation zone and σ_x is still the most potential stress to cause cracking of RCC. This result indicates the expansion of the separation zone will accelerate the occurrence and propagation of the longitudinal cracking. When the load is away from the slab edge, the influence of the separation zone become weak. In general, the expansion of the separation zone caused by pumping intensifies the potential of longitudinal cracking.

By directly comparing the slope term in the developed fatigue models (i.e., 9.071 for equation (8) and 9.507 for equation (9)), a thicker RCC pavement will have a longer fatigue life than a thinner RCC pavement under a same stress ratio. This implies that, by considering the critical flexural stress alone, the predicted fatigue life of a 4 in. thin RCC pavement will be over-estimated if equation (9) is used, and vice versa. Therefore, when performing a thickness design for a thin RCC pavement, the RCC slab thickness needs to be considered in the fatigue analyses due to possible reduced overall structural loading capacity. The results of

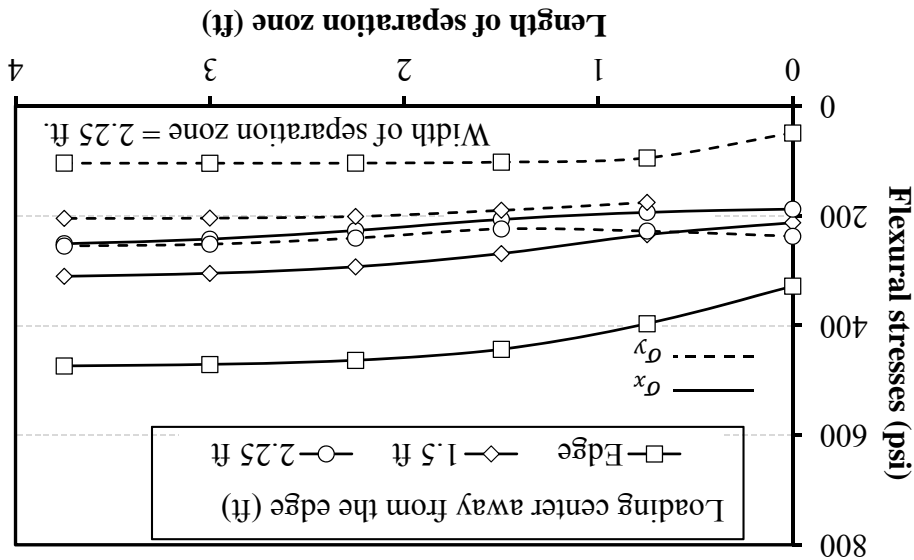
For sections 3 & 6: $\log N_f = 9.071 - 12.729 \times SR$ (8)

For sections 2 & 5: $\log N_f = 9.507 - 12.597 \times SR$ (9)

A fatigue analysis was conducted in this study based on the cracking performance obtained on the failed RCC Sections of 2, 3, 5, and 6. The following two fatigue equations were obtained, in which N_f is the allowable number of fatigue load repetitions and the critical (maximum) flexural stress under wheel load divided by flexural strength of the concrete slab is defined as the stress ratio (SR). The field critical tensile stresses used in the analysis were estimated from the obtained instrumentation responses (13).

Fatigue Cracking and Failure Mechanism on Thin RCC Pavements

Figure 36 Maximum flexural stresses versus length of separation zone



this APT study further confirm that the current literature fatigue question for the thickness design of industrial pavements cannot be used in the fatigue analysis of thin RCC pavements.

According to the results of post mortem trenches and the above critical flexural stress analysis, a hypothesis of the failure mechanism was developed on a thin RCC pavement:

- Fatigue cracks can be generated at the bottom of saw-cut joints over weak subgrade area and will eventually propagate to the surface (i.e., transverse cracking).
- After the crack-through of the saw-cut joint, the potential cracking initiates at the bottom of the slab within the wheel path along the longitudinal direction of the thin RCC slab.
- Then, pumping and erosion after raining becomes a serious issue, which causes the loss of the fine materials from the stabilized soil base and subsequently creates a separation zone or voids below the RCC slab. The voids will accelerate the propagation of the longitudinal cracking at the bottom of the slab within the wheel path.
- After the substantial propagation of the longitudinal cracking along the wheel path, the pavement may be viewed as two separate slabs and the wheel loading can be considered as an edge loading. Similar to the longitudinal cracking, fatigue transverse cracking will initiate at the bottom of the slab perpendicular to the wheel moving direction.
- After the propagation of the transverse cracking and the expansion of the voids, the slab can be further considered as many small cantilever slabs. With the wheel load applied at the free end (i.e., cracked wheel path), the fixed end of the cantilever slab will have a top-down cracking potential and eventually top-down cracking will generate outside the loading area and parallel to the wheel path.
- In reality, the propagation of these longitudinal cracking, transverse cracking, bottom-up cracking and top-down cracking may not exactly occur one after another by following the steps as described above; however, the described propagation of the cracking summarizes basic mechanism of the thin RCC cracking performance under the accelerated repeated loading.

Procedure for Thin RCC Pavement Design

RCC pavement thickness design falls into two categories: one for heavy-duty industrial pavements (e.g., ports and multimodal terminals) and the other for pavements carrying mixed-vehicle traffic (e.g., different sizes and weights of roadway-licensed trucks and lighter

vehicles). For heavy-duty industrial pavements, the RCC thickness design may be based on the expected number of load repetitions of the single heaviest vehicle, whereas other vehicles of significantly lighter weight can be ignored. Such an approach is used in both the RCC-Pave and USACE's RCC pavement design procedures. For RCC pavements designed to carry mixed highway traffic vehicles, the design procedures for un-doweled conventional concrete pavements (e.g., the ACI tables or ACPA's StreetPave computer program) may be used. However, the fatigue models developed for the conventional PCC or industrial RCC pavements have been found in this study not appropriate for thin RCC pavements. Therefore, a thickness design procedure specifically for the design of thin RCC-surfaced pavement structure is presented in the following section. The primary design factors include the design period, design traffic (including load safety factor, axle load distribution), flexural strength of RCC (or the modulus of rupture of RCC), and the modulus of subbase-subgrade reaction, k . Other inputs are the elastic modulus of RCC and Poisson's ratio. A widen lane design (i.e., >14-ft. wide) is considered in the procedure in lieu of a tied shoulder or curb. The proposed procedure is based on the Portland Cement Association's thickness design method (or PCA method), in which both the fatigue analysis and erosion analysis will be considered.

Design Period and Traffic Inputs

The design period has a direct impact to thickness design. Selection of the design period (or the RCC pavement design life) for a specific project is based on engineering judgment, economic analysis of pavement costs and service level. For a thin RCC-surfaced pavement used for a low volume road, 15 to 20 years may be selected.

The design period dictates the number of trucks and traffic loading required for the pavement. In the proposed design procedure, the traffic load spectra (or axle load distributions) as recommended in the PCA method are considered [28]. The axle load distributions consist of the number of load repetitions of each axle load (i.e., single, tandem, tridem, and quad axles) per 1000 trucks within the total axle applications. Other traffic inputs required are the average daily traffic (ADT), annual growth rate, percentage of truck, and proportion of truck in design lane.

Failure Criteria

For the thickness design procedure of thin RCC surfaced pavements, both fatigue and erosion analyses will be considered. Cumulative damage criterion is used for the fatigue analysis to prevent a total area of fatigue cracking under 40% during the design period. The principal consideration of erosion analysis is to prevent pavement failures such as pumping, erosion of

foundation, and joint faulting due to critical corner deflections during the design period [28].

Fatigue Analysis. The fatigue analysis is based on Miner's cumulative fatigue damage assumption [29]. The procedure requires the estimation of load-induced critical tensile stress under an RCC slab for each axle load and axle type, and the maximum allowable load repetitions (N_f) under each axle load group during the design period. The fatigue models developed for thin RCC pavements in this study are used in the determination of the maximum allowable load repetitions (N_f); whereas, the PCA's equivalent stress concept (the maximum edge bending stress of a concrete slab) is used in the estimation of the load-induced critical tensile stress of thin RCC slab. The determination of equivalent stress in PCA method is based on the maximum edge bending stress, estimated from J-SLAB finite element analysis under a single axle (SA) load and a tandem axle (TA) load for different levels of slab thickness and modulus of subgrade reaction [30]. The following equation is presented in the PCA method [31]. Due to the load-induced critical stresses in thin RCC pavement are found located at the bottom of RCC slab along saw-cut joints, the equivalent critical stress estimated by the PCA equation needs to be adjusted by an adjustment factor of 0.6. Note that the critical stress adjustment factor was determined and validated with the ATLaS loading results obtained in the APT experiment.

$$\sigma_{eq} = \frac{6 * M_e}{h^2} * f_1 * f_2 * f_3 * f_4 \quad (10)$$

$$M_e = \begin{cases} -1600 + 2525 * \log(l) + 24.42 * l + .204 * l^2 & SA/NS \\ 3029 + 2966.8 * \log(l) + 133.63 * l - .0632 * l^2 & TA/NS \\ (-970.4 + 1202.6 * \log(l) + 53.587 * l) * (.8742 + .01088 * k^{0.447}) & SA/WS \\ (2005.4 - 1980.9 * \log(l) + 99.008 * l) * (0.8742 + 0.01088 * k^{0.447}) & TA/WS \end{cases}$$

$$f_1 = \begin{cases} \left(\frac{24}{SA}\right)^{0.06} * \left(\frac{SA}{18}\right) & SA \\ \left(\frac{48}{TA}\right)^{0.06} * \left(\frac{TA}{36}\right) & TA \end{cases}$$

$$f_2 = \begin{cases} 0.892 + \frac{h}{85.71} - \frac{h^2}{3000} & NS \\ 1 & WS \end{cases}$$

$$f_3 = 0.894 \text{ for } 6\% \text{ truck at the slab edge}$$

$$f_4 = \frac{1}{[1.235 * (1 - CV)]}$$

$$l = (E * h^3 / ((12 * (1 - \mu^2) * k)))^{0.25}$$

where,

σ_{eq} =PCA equivalent stress

h=trial thickness

k=modulus of subgrade reaction

SA= Single Axle Load

TA= Tandem Axle Load

NS= No Shoulder

WS= With Shoulder

CV=One coefficient of variation, PCA recommend CV=15%

E= Modulus of Elasticity

μ = Poisson's Ratio

l= Radius of relative stiffness

Once the allowable number of load repetition N_f is estimated based on the equivalent stress analysis, the percentage of fatigue damage for each axle load and axle type will then be calculated by dividing N_f to the expected number of load repetitions. The total cumulative fatigue damage has to be within the specified 100% limiting design criterion, or a different trial slab thickness has to be used. The following equations will be used to calculate the fatigue damage for each axle type and load group.

$$FD = \frac{n}{N_f} \quad (11)$$

$$FD_{total} = FD_{Single} + FD_{Tandem} + FD_{Tridem} \quad (12)$$

Erosion Analysis. Another principal mode of failure for concrete pavement is pumping or erosion of base/subbase underneath a concrete slab. In the proposed thickness design procedure, the PCA's erosion analysis procedure is recommended. PCA's erosion analysis concept is to avoid pavement failures due erosion which is closely related to pavement deflection. The most critical pavement deflection occurs at the slab corner when an axle load is placed at the joint near to the corner [28]. The following equations are used in the PCA method in determination of equivalent corner deflection (δ_{eq}).

$$\delta_{eq} = \frac{P_c}{k} * f_5 * f_6 * f_7 \quad (13)$$

$$P_c = \begin{cases} 1.571 + \frac{46.127}{l} + \frac{4372.7}{l^2} - \frac{22886}{l^3} & SA/NS \\ 1.847 + \frac{213.68}{l} - \frac{1260.8}{l^2} + \frac{22989}{l^3} & TA/NS \\ 0.5874 + \frac{65.108}{l} + \frac{1130.9}{l^2} - \frac{5245.8}{l^3} & SA/WS \\ 1.47 + \frac{102.2}{l} - \frac{1072}{l^2} + \frac{14451}{l^3} & TA/WS \end{cases}$$

$$f_5 = \begin{cases} \left(\frac{SA}{18}\right) & SA \\ \left(\frac{TA}{36}\right) & TA \end{cases}$$

$$f_6 = \begin{cases} 0.95 & NS \\ 1.001 - \left(0.26363 - \frac{k}{3034.5}\right)^2 & WS \end{cases}$$

$$f_7 = \begin{cases} 0.896 & NS \\ 1 & WS \end{cases}$$

The PCA concept is that a thin slab with a shorter deflection basin receives a faster load punch than a thicker slab. The following equations were developed to compute the allowable load repetitions:

$$\log N_e = 14.524 - 6.777 * (C_1 * P - 9)^{0.103} - \log C_2 \quad \begin{matrix} C_1 * P > 9 \\ C_1 * P \leq 9 \end{matrix} \quad (14)$$

$$N_e = \text{unlimited}$$

$$P = 268.7 * \left(\frac{k^{1.27} * \delta_{eq}^2}{h}\right)$$

$$EF = \log \left[\frac{11111 * (0.896 * P)^2 * C_1}{h * k^{0.73}} \right]$$

$$C_1 = 1 - \left(\frac{k}{2000} * \frac{4}{h}\right)^2$$

$$C_2 = \begin{cases} 0.06 & NS \\ 0.94 & WS \end{cases}$$

where,

N_e = Allowable number of repetitions

P= Rate of work or Power

EF= Erosion Factor

C1 = adjustment factor; 1 for untreated subbases and 0.9 for stabilized subbases

C2 = shoulder adjustment factor

SA= Single Axle Load

TA= Tandem Axle Load

The equation for erosion damage is

$$\text{Percent erosion damage} = 100 * \sum_{i=1}^m \frac{n_i}{N_e} \quad (15)$$

In which m is the total number of load groups, n_i is the predicted number of repetitions for the i th load group, and N_e is the allowable number of repetitions for the i th load group.

The erosion potential would decrease with the use of a stabilized base layer, dowelled transverse joints, and tied concrete shoulders. Due to the use of soil cement or cement treated base layer, there is lack of evidence of erosion as a failure mode for RCC test sections investigated. However, the above PCA erosion analysis method is adopted to check the potential erosion damage for a designed thin RCC pavement structure.

Design Spreadsheet

A user-friendly Excel spreadsheet has been developed in this study for thin RCC-surfaced pavement design. Generally speaking, the proposed method is similar to the PCA's design methodology for un-doweled jointed plain concrete pavements. The primary difference is the design fatigue equation used. In the proposed design procedure, a more suitable fatigue equation for thin RCC slabs is considered. Figure 37 presents a flowchart for the proposed design procedure.

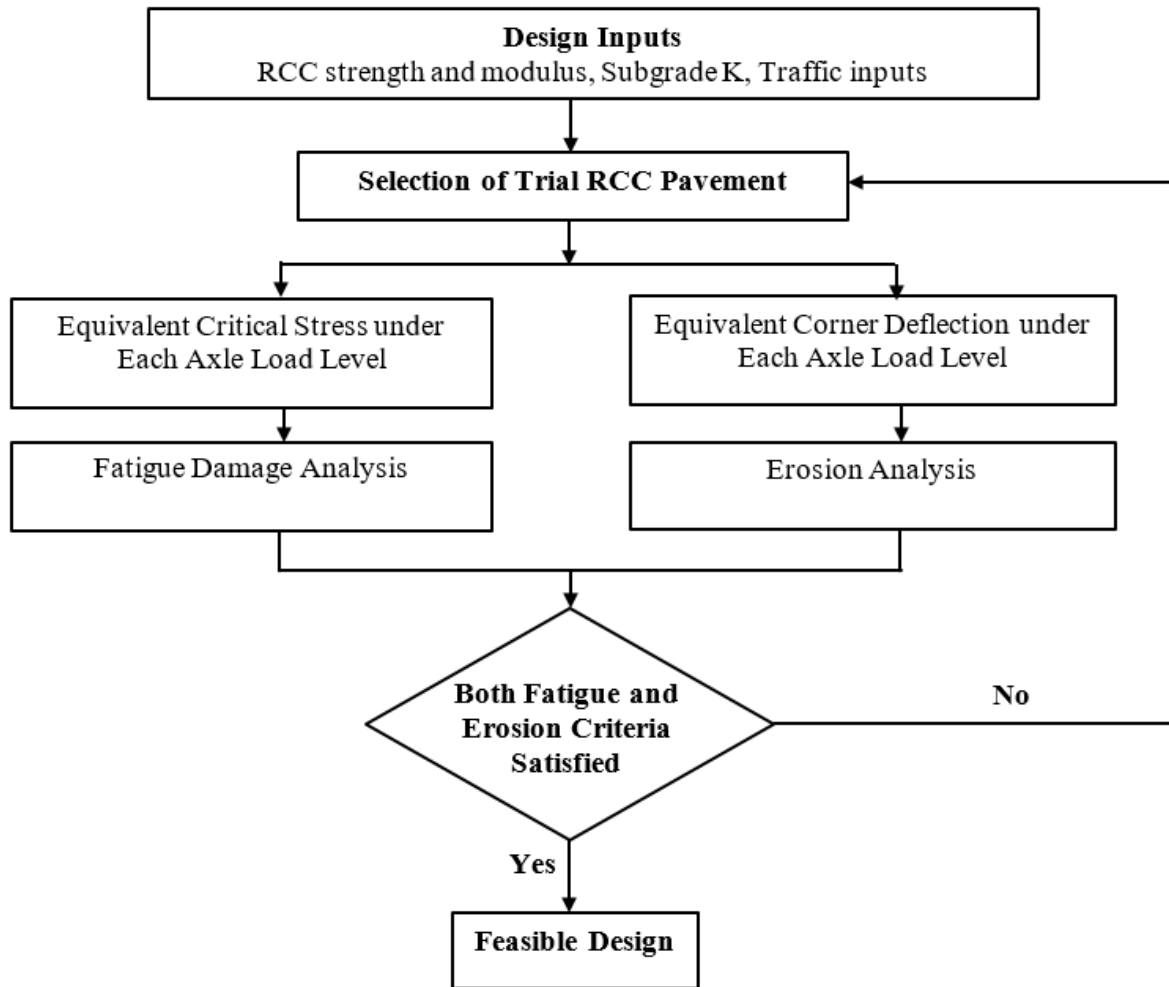


Figure 37
The flowchart of the proposed thin RCC design procedure

Design Example

A low volume pavement structure design is presented in the following example. The proposed pavement structure includes a thin RCC slab over an 8.5-in. soil cement base built over a 12-in. cement-treated soil subgrade. The pavement in the design carries an ADT of 3000 with 25% truck traffic. An assumed axle load distributions are listed in Table 8. The pavement design life is for 15 years. Other design inputs are shown below:

| | |
|---|------------|
| RCC modulus of rupture (MR) | = 661 psi |
| RCC modulus of elasticity | = 4000 ksi |
| RCC Poisson's ratio | = 0.15 |
| Subgrade and Subbase combined support (k) | = 350 pci |

Design Traffic:

| | |
|--------------------------|--|
| 2-way ADTT | = 750 |
| Growth Rate | = 2% |
| Directional Distribution | = 50% |
| Design Lane Distribution | =100% |
| Traffic Category | = Low Volume Road with Heavy Truck Traffic |

Table 8
Example load distribution of traffic axle loads

| Axle Load, kip | Axles/1000 | Axle Load, kip | Axles/1000 | Axle Load, kip | Axles/1000 |
|---------------------------|-------------------|---------------------------|-------------------|---------------------------|-------------------|
| Single Axles | | Tandem Axles | | Tridem Axles | |
| 34 | 0 | 60 | 0 | 78 | 0 |
| 32 | 0 | 56 | 0 | 72 | 0 |
| 30 | 0 | 52 | 0 | 66 | 0 |
| 28 | 0 | 48 | 0 | 60 | 0 |
| 26 | 0.5 | 44 | 0.5 | 54 | 0 |
| 24 | 1 | 40 | 1 | 48 | 0 |
| 22 | 2 | 36 | 3 | 42 | 0 |
| 20 | 3 | 32 | 20 | 36 | 0 |
| 18 | 5 | 28 | 50 | 30 | 0 |
| 16 | 15 | 24 | 200 | 24 | 0 |
| 14 | 40 | 20 | 1000 | 18 | 0 |
| 12 | 150 | 16 | 2500 | 12 | 0 |
| 10 | 400 | 12 | 4000 | 6 | 0 |
| 8 | 800 | 8 | 5500 | 0 | 0 |
| 6 | 1500 | 4 | 7000 | 0 | 0 |
| 4 | 3000 | 0 | 0 | 0 | 0 |

The proposed RCC thickness design procedure (i.e., the design Excel spreadsheet) was used. A designed RCC slab thickness was found to be 5-in. Detailed fatigue and erosion analyses are showed in Table 9. As can be seen in Table 9, the pavement design is based on the fatigue damage control, in which the accumulated fatigue damage is approximately 98.3% with the accumulated erosion damage of 87.9% when a RCC thickness is set to be 4.95 in. Continuously decreasing the RCC thickness would increase both the fatigue and erosion damage significantly. Therefore, a 5-in. RCC slab thickness may be considered as the design thickness.

Table 9
Fatigue and erosion analysis results for proposed design

| Axle Load (kip) | Expected No. of Load Repetition | Stress Ratio | Allowable No. of Load Repetition | %Fatigue Damage | %Erosion Damage |
|------------------------|--|---------------------|---|------------------------|------------------------|
| Single Axles | | | | | |
| 34 | 0 | 0.57 | 220 | 0.00 | 0.00 |
| 32 | 0 | 0.54 | 550 | 0.00 | 0.00 |
| 30 | 0 | 0.51 | 1375 | 0.00 | 0.00 |
| 28 | 0 | 0.47 | 3454 | 0.00 | 0.00 |
| 26 | 1185 | 0.44 | 8710 | 13.61 | 5.72 |
| 24 | 2370 | 0.41 | 22054 | 10.75 | 7.26 |
| 22 | 4741 | 0.38 | 56106 | 8.45 | 8.81 |
| 20 | 7111 | 0.35 | 143465 | 4.96 | 7.54 |
| 18 | 11851 | 0.31 | 368928 | 3.21 | 6.61 |
| 16 | 35554 | 0.28 | 954745 | 3.72 | 9.23 |
| 14 | 94811 | 0.25 | 2488574 | 3.81 | 9.32 |
| 12 | 355542 | 0.21 | 6540459 | 5.44 | 8.43 |
| 10 | 948112 | 0.18 | 17358168 | 5.46 | 0.43 |
| 8 | 1896223 | 0.15 | 46617921 | 4.07 | 0.00 |
| 6 | 3555418 | 0.11 | 127103676 | 2.80 | 0.00 |
| 4 | 7110837 | 0.08 | 353786228 | 2.01 | 0.00 |
| Tandem Axles | | | | | |
| 60 | 0 | 0.43 | 10962 | 0.00 | 0.00 |
| 56 | 0 | 0.41 | 24166 | 0.00 | 0.00 |
| 52 | 0 | 0.38 | 53456 | 0.00 | 0.00 |
| 48 | 0 | 0.35 | 118679 | 0.00 | 0.00 |
| 44 | 1185 | 0.32 | 264540 | 0.45 | 1.47 |
| 40 | 2370 | 0.30 | 592264 | 0.40 | 1.66 |
| 36 | 4741 | 0.27 | 1332445 | 0.53 | 2.56 |
| 32 | 7111 | 0.24 | 3014003 | 1.57 | 7.62 |
| 28 | 11851 | 0.21 | 6859840 | 1.73 | 6.56 |
| 24 | 35554 | 0.18 | 15724246 | 3.01 | 4.68 |
| 20 | 94811 | 0.15 | 36346604 | 6.52 | 0.00 |
| 16 | 355542 | 0.13 | 84875382 | 6.98 | 0.00 |
| 12 | 948112 | 0.10 | 200783411 | 4.72 | 0.00 |
| 8 | 1896223 | 0.07 | 483482492 | 2.70 | 0.00 |
| 4 | 3555418 | 0.03 | 1197357392 | 1.39 | 0.00 |
| Total | | | | 98.3% | 87.9% |

Construction Cost Analysis

To quantify cost benefits from using a thin RCC pavement in lieu of an asphalt pavement alternative for roadways where heavy and/or overloaded trucks are often encountered, a construction cost analysis was performed on two pavement structure alternatives. As outlined in Figure 38, Alternative A contains a pavement structure obtained in the aforementioned design example (i.e., 5-in. RCC and 8.5-in. soil cement over a 12-in. cement-treated subgrade); whereas, Alternative B has a similar base and subgrade structure as alternative A but uses a 7-in. hot mix asphalt (HMA) as the surface layer. According to the 1993 AASHTO design guide, the pavement structure of the alternative B would be expected to have a pavement life of one million of 18-kip equivalent single axle load (ESAL), when the layer coefficients of a new HMA and a soil cement layers are assumed to be 0.44 and 0.14, respectively. According to the axle load distribution used in the previous RCC pavement design example, the total estimated ESALs based on the 1993 flexible pavement equivalent load factors (EALF) would be 1.35 million. That means, the pavement life of the Alternative B is less than that estimated for the Alternative A. Thus, using the 7-in. HMA thickness as compared to a 5-in. RCC is still a conservative consideration. Note that no structural value was assigned to a cement-treated “working table” layer based on engineering judgment.

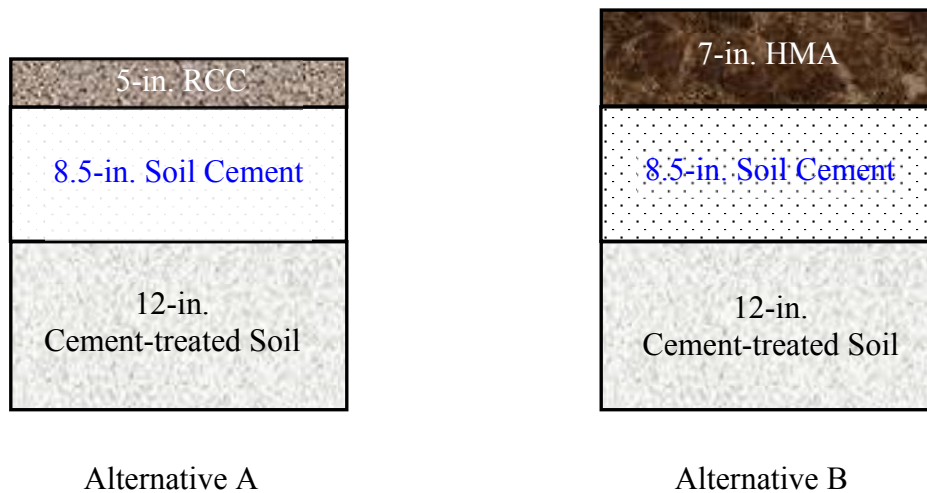


Figure 38
Pavement alternatives used in cost-benefit analysis

The construction costs of two pavement alternatives are listed in Table 10. The unit prices in the table were determined from the previous construction costs and APT experiments. The

quantities were calculated based on a 13-ft. wide lane for one-mile long. As shown in Table 10, the estimated construction costs for Alternatives A and B were \$198,082 and \$311,169.00 respectively. Therefore, by using a 5-in. RCC in lieu of a 7-in. HMA layer, the estimated cost benefits would be \$113,087 per lane mile. Applying the estimated cost benefits to a typical 2-lane, 10-mile long roadway project, the use of a 5-in. RCC layer in lieu of a 7-in. HMA layer results in a total construction cost savings up to \$2,261,740.

Table 10
Initial construction costs

| <u>Alternative A</u> | | | |
|----------------------------------|---------------------------|------------------------|------------------------|
| Materials | Unit Prices (\$) | Quantity | Construction Costs(\$) |
| 5-in. RCC | \$115 per yd ³ | 1059.3 yd ³ | 121,815.00 |
| 8.5-in. Soil Cement | \$10 per yd ² | 7626.7 yd ² | 76,267.00 |
| Total Initial Construction Costs | | | \$198,082.00 |
| <u>Alternative B</u> | | | |
| Materials | Unit Prices (\$) | Quantity | Construction Costs(\$) |
| 7-in. HMA | \$80 per ton | 2936.3 ton | 234,902.00 |
| 8.5-in. Soil Cement | \$10 per yd ² | 7626.7 yd ² | 76,267.00 |
| Total Initial Construction Costs | | | \$311,169.00 |

CONCLUSIONS

Six full-scale RCC pavement sections, including three RCC slab thicknesses (4, 6, and 8 in.) with two cement stabilized/treated soil bases, were tested under an APT experiment. In the end, four thinner RCC pavement sections were severely damaged due to the fatigue cracking. Results of the crack-mapping and post mortem trenches indicated that a thin RCC pavement would be cracked initially along a longitudinal direction under the repetitive traffic loading. A finite difference model was developed to assess the cracking potential for a thin RCC pavement. The following observations and conclusions may be drawn from this study:

- All RCC sections received a significantly large amount of heavy truck loads in this APT study indicating that a thin RCC pavement would have outstanding load carrying capacity to be used for low-volume roadways with significantly heavy truck traffics when properly constructed;
- Four relatively-thin RCC sections (with a thicknesses of 4- and 6-in.) were able to be loaded to failure with a fatigue cracking mode. The fatigue cracks were initially observed on pavement surface in the longitudinal direction within the tire print. With continuous load repetitions and the crack pumping actions, voids could be formed underneath a RCC slab, which generated more deflections and propagate cracks into a fatigue cracking failure;
- Post-mortem trench results observed that the fatigue cracks could be generated from the bottom or top of a thin RCC slab as well as on a saw-cut joints location. Numerical simulation results revealed that the critical stresses would be located at the bottom of RCC slab along saw-cut joints. In addition, weak subgrade areas would be the prone locations for pavement cracking.
- Based on the forensic results and critical flexural stress analysis, a load-induced cracking failure mechanism of thin RCC-surface pavement was proposed. Basically, a thin RCC slab under traffic and environmental loading would be fatigue-failed due to a combination of both propagations of longitudinal and transverse cracks as well as pumping effect. After the substantial propagation of the longitudinal cracking along the wheel path, the pavement may be viewed as two separate slabs and the wheel loading can be considered as an edge loading.
- A thickness design procedure with an Excel-based design spreadsheet specifically for the design of thin RCC-surfaced pavement structure was proposed in this study. The proposed procedure, based on the PCA's design methodology for un-doweled jointed plain concrete pavements, considers both the fatigue analysis and erosion analysis with a tied-shoulder. The primary design factors include the flexural strength of RCC,

the modulus of subbase-subgrade reaction, the axle load distributions, and thin RCC fatigue model.

- An initial construction cost analysis was performed between two pavement design alternatives: one with a 5-in. RCC slab and the other having a 7-in. HMA top layer. Both pavement structures was designed with a pavement life more than 1 million EASLs over a 15-year design period. By using a thin RCC in lieu of a HMA layer, the estimated initial construction cost savings would be \$113,087 per lane mile and \$2,261,740 for a typical 2-lane, 10-mile long roadway project.

RECOMMENDATIONS

It is recommended that the Pavement Design Section begin implementing a new pavement design alternative of using a thin RCC-surfaced pavement structure for DOTD's low-volume roadways where heavy (and overloaded) trucks are often encountered. The recommended pavement structure consists of a thin RCC slab (usually 4~6 in.) built over a soil cement or cement treated base layer. The thickness design procedure provided in this study may be used in determination of the design RCC thickness. The RCC job mix formula (JMF) should have similar material compositions and gradation as those considered in this study, except that more fine aggregates and natural sands should be used in order to achieve the design roadway density and a rideable pavement surface (e.g., IRI = 100~120 in/mile). If the RCC pavement structure is to be used for high volume roadways, surface diamond grinding or a thin asphalt overlay is recommended. A draft RCC construction specification is attached in Appendix B.

ACRONYMS, ABBREVIATIONS, AND SYMBOLS

| | |
|--------|--|
| AASHTO | American Association of State Highway and Transportation Officials |
| ACI | American Concrete Institute |
| ACPA | American Concrete Pavement Association |
| ADT | Average Daily Traffic |
| ADTT | Average Daily Truck Traffic |
| APT | Accelerated Pavement Testing |
| DOTD | Department of Transportation and Development |
| FHWA | Federal Highway Administration |
| FWD | Falling Weight Deflectometer |
| JDMD | Joint Deflection Measurement Device |
| JMF | Job Mix Formula |
| LTRC | Louisiana Transportation Research Center |
| LVDT | Linear Variable Differential Transformer |
| RCC | Roller Compact Concrete |
| SA | Single Axle |
| PCA | Portland Cement Association |
| TA | Tandem Axle |
| TDR | Time Domain Reflectometer |
| UCS | Unconfined Compressive Strength |
| USACE | United States Army Corps of Engineering |
| in. | Inch |
| ft. | Feet |

REFERENCES

1. Gauthier, P. and Marchand, J. *Design and Construction of Roller-Compacted Concrete Pavements in Quebec*. Quebec, Canada: Department of Civil Engineering, Laval University, 2005.
2. Nanni, A., Ludwig, D., and Shoenberger, J. "Roller Compacted Concrete for Highway Pavements." *Concrete International*, Vol. 18, No. 5, 1996, pp. 33-38.
3. Palmer, W. D. "Paving with Roller Compacted Concrete." *Public Works*, January 2005, pp.41-45
4. Kim, Y.S. "Roller-Compacted Concrete Shoulder Construction on an Interstate Highway in Georgia." Presentation at the Transportation Research Board 2007 Annual Meeting. Washington, D.C
5. Piggot, R. W. *Roller Compacted Concrete Pavements – A Study of Long Term Performance*. RP366, Portland Cement Association, 1999.
6. Harrington, D., Abdo, F., Adaska, W., and Hazaree, C. *Guide for Roller-Compacted Concrete Pavements*. National Concrete Pavement Technology Center, Institute for Transportation, Iowa State University, 2010.
7. U.S. Army Corps of Engineers (USACE). *Roller-Compacted Concrete*. USACE Engineer Manual EM 1110-2-2006, 2000.
8. Portland Cement Association (PCA). *Guide Specification for Construction of Roller-Compacted Concrete Pavements*. PCA Document IS009, 2004.
9. Personal email communication on 2012 with Mr. Wayne S. Adaska at Portland Cement Association, Skokie, Illinois.
10. ACI COMMITTEE 325.10R-95, "State-of-the-Art Report on Roller-Compacted Concrete Pavements, Manual of Concrete Practice." American Concrete Institute, 1995.
11. Ambrose, J. Beating Asphalt on Price, *Concrete Producer*, March 2002.
12. Dufferin Construction Company, *Roller Compacted Concrete Pavements*.
13. U.S. Army Corps of Engineers (USACE). *Roller-Compacted Concrete Pavement Design and Construction*. Technical Letter ETL 1110-3-475, 1995.
14. Delatte, N. Simplified Design of Roller-Compacted Concrete Composite Pavement. In *Transportation Research Record: Journal of the Transportation Research Board*, No. 1896, TRB, National Research Council, Washington, D.C., 2004, pp.57-65.
15. Zollinger, C. "Recent Advances and Uses of Roller Compacted Concrete Pavements in the United States." *Paving Solutions*, CEMEX, Inc, Houston, TX USA, 2015
16. The National RCC explorer, web: www.rcc.acpa.org, Date accessed: March 2016
17. ASTM D1557 "Standard Test Methods for Laboratory Compaction Characteristics of Soil Using Modified Effort (56,00 ft-lbf/ft³ (2,700 kN-m/m³))." *Annual Book of ASTM Standards*, Vol. 04.08, ASTM, Philadelphia, PA, 2013.

18. ASTM C1435 “Standard Practice for Molding Roller-Compacted Concrete in Cylinder Molds Using a Vibrating Hammer.” *Annual Book of ASTM Standards*, Vol. 04.02, ASTM, Philadelphia, PA, 2013.
19. ASTM C39 “Standard Test Method for Compressive Strength of Cylindrical Concrete Specimens.” *Annual Book of ASTM Standards*, Vol. 04.02, ASTM, Philadelphia, PA, 2013.
20. Louisiana Transportation Research Center. “Roller Compacted Concrete Study First to Use New Concrete Testing Device.” *Technology Today*, Vol. 28, No. 3, 2014.
21. Rapid International Ltd. *Rapidmix 400C*, www.thomaco.com/pdf/rapidmix400cen.pdf. Last accessed on July 28, 2014.
22. Huang, Y.H. *Pavement Analysis and Design*. Prentice-Hall, Engle-wood Cliffs, NJ, 1993
23. Chang, G. K. and Rasmussen. R. O. *FHWA ProVAL User’s Guide Version 2.73*. The Transtec Group, Inc. Austin, TX., 2007.
24. Drenth, K., ELMOD 6: The Design and Structural Evaluation Package for Road, Airport and Industrial Pavements. *8th International Conference on Concrete Block Paving*, San Francisco, California, 2006.
25. Wu, Z., King, B., Abadie, A., and Zhang, Z. “Development of a Design Procedure for Prediction of Asphalt Pavement Skid Resistance.” *Transportation Research Record: Journal of the Transportation Research Board*, No.2306, Transportation Research Board of the National Research Council, Washington, D.C., 2012, pp. 161-170.
26. Damrongwiriyapap, N., Liang, Y., and Xi, Y. “Application of Roller Compacted Concrete in Colorado’s Roadways.” Report No. CDOT-2012-11, Colorado Department of Transportation – Research, Denver, CO, 2012.
27. Williams, S. G. “Construction of Roller Compacted Concrete Pavement in the Fayetteville Shale Play Area.” *Transportation Research Record: Journal of the Transportation Research Board*, No. 2408, Transportation Research Board of the National Research Council, Washington, D.C., 2014, pp. 47-54.
28. Portland Cement Association. *The Design for Concrete Highway and Street Pavements*. PCA, Skokie, IL, U. S. A. (1984)
29. Miner, M.A. “Cumulative Damage in Fatigue.” *Trans. ASME*, Vol. 67, 1945
30. Tayabji, S. and Dand Colley, B. E., “Analysis of Jointed Concrete Pavement,” Report No. FHWA-RD-86-041, Federal Highway Administration, 1986.
31. Ying-Haur L. and Carpenter, S. PCAWIN Program for Jointed Concrete Pavement Design. *Tamkang Journal of Science and Engineering*.2001. 4(4): 293-300.

APPENDIX A

Loading Sequence

Figure 39 presents the loading sequence and the corresponding predicted ESAL numbers for Section 6 (4+8.5RCC). This section began the wheel loading by the loading sequence of 9, 16, 20, 22, and 25 kips, then tested under the 16-kip wheel load till to fatigue failure. The total estimated ESALs is approximately 19.2 million.

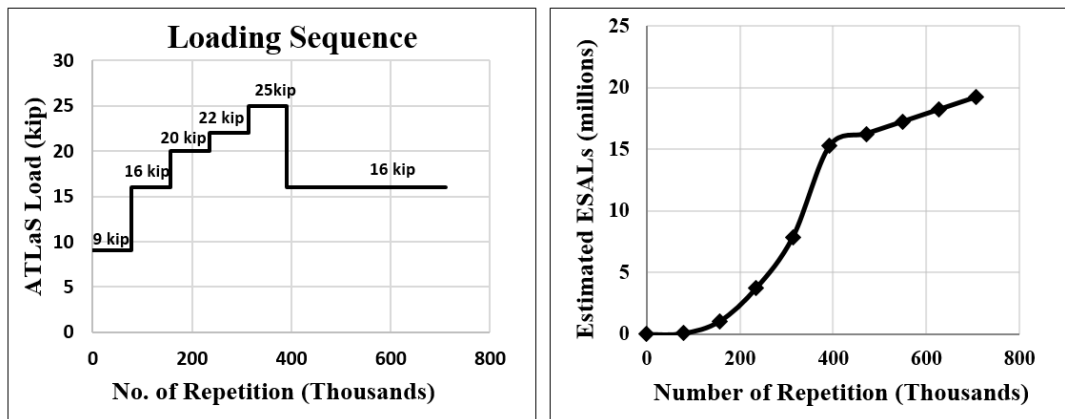


Figure 39

Loading sequence and corresponding ESALs for Section 6 (4+8.5RCC)

Section 6 (4+8.5RCC)

Figure 40 shows the cracking development under different load repetitions observed on this section. FWD backcalculated subgrade moduli (M_r) at different stations were also plotted on a vertical axis to the left side in Figure 40. Neither visible nor measurable distresses could be obtained on this section at the ends of 9-kip, 16-kip, and 20-kip of ATLaS dual-tire loading. At the beginning of the 22-kip loading, a hairline longitudinal crack around Station+10 was noticed, which was in the middle of one tire print, Figure 40. With additional load repetitions, the longitudinal crack propagated and expanded continuously, and resulted in some pumping fine materials through the cracks and saw-cut joints on this section. After 480,000 load repetitions, longitudinal cracks from outside the wheel path started to initiate. Finally, the inside and outside longitudinal cracks connected to each other and a punchout type failure occurred around Station+15 after a total of 706,500 passes of ATLaS dual tire loading. Interestingly, the cracking failure was observed confined only in the first half of the loading area on Section 6 (4+8.5RCC) (Figure 40).

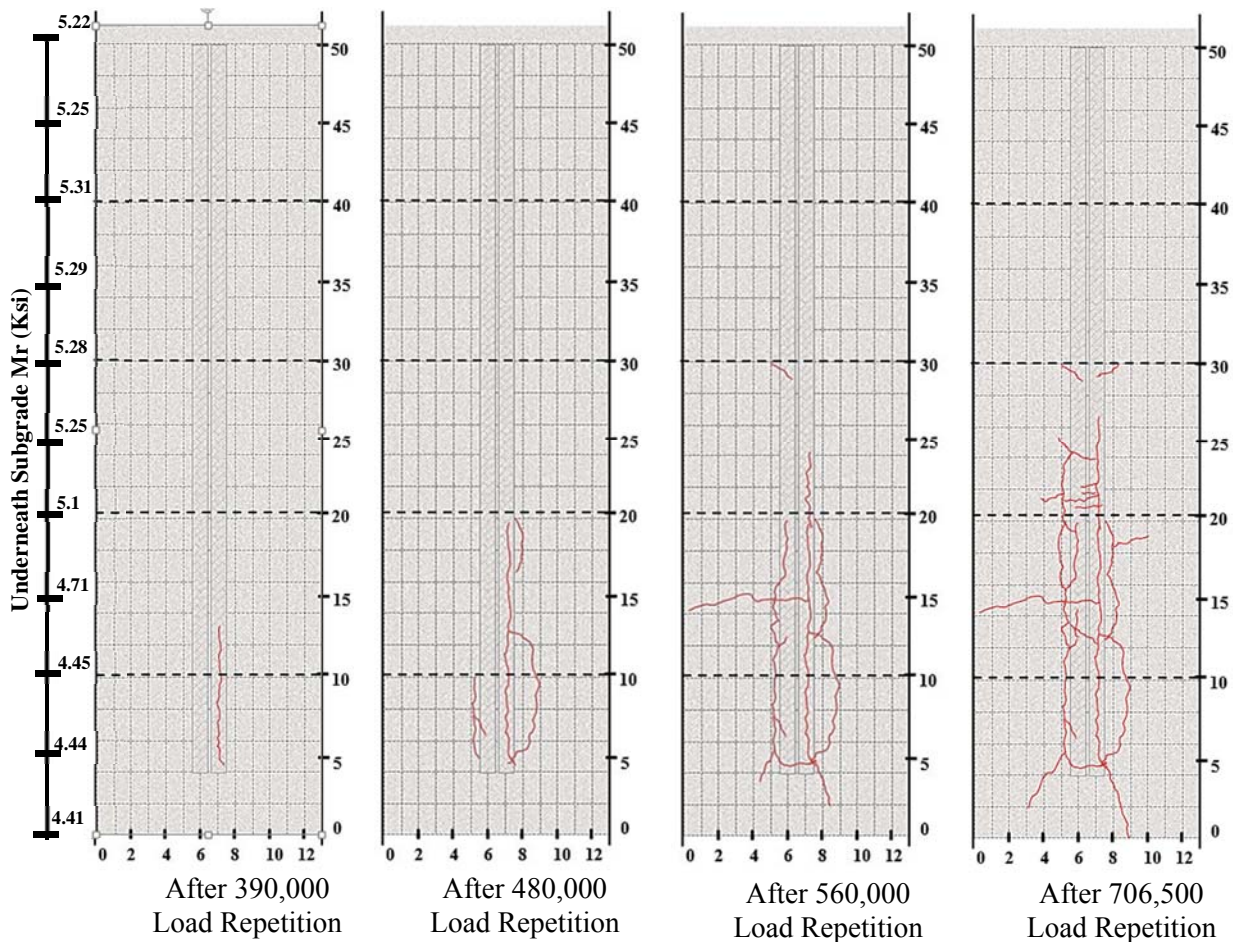


Figure 40
Cracks vs. load repetitions for Section 6 (4+8.5RCC)

The following findings were found: (1) the initial longitudinal cracking observed in the middle of one tire print seems to be a bottom-up crack due to high tensile stresses at the bottom of the 4-in. RCC slab; (2) The weaker subgrade portion under the loading area caused a higher tensile stress under the slab than did the stronger subgrade portion; (3) with continuous load repetitions and more pumping of fine materials, voids would be formed underneath the slab, which generated more deflections and cracks of the slab under loading; and (4) due to only 4 in. of slab thickness, the final cracking pattern was kept in a narrow area, different from the cracking pattern observed on the 6 in. RCC section to be described below.

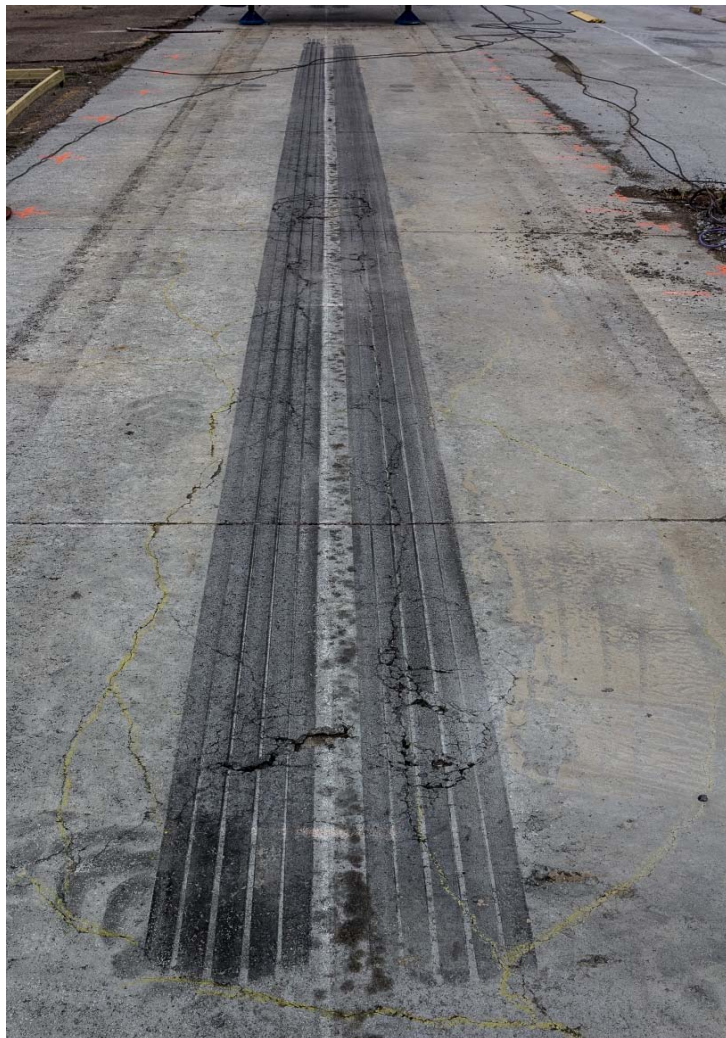


Figure 41
Distresses observed on Section 6 (4+8.5RCC)

Section 5 (6+8.5RCC)

It took much longer and more loading repetitions to fail this section than Section 6 (4+8.5RCC). A total of 1,750,850 load repetitions of various loads was applied on this section and the estimated ESALs to the fatigue failure was 87.4 million. Figure 42 shows the cracking development under different load repetitions observed on Section 5 (6+8.5RCC). Similar to the Section 6 (4+8.5RCC), the crack was also initiated in longitudinal direction in this section. However, this time the longitudinal cracking was initiated along the edge of a wheel tire. Another major difference between the two sections is that the cracking pattern was much wider in Section 5 (6+8.5RCC) than Section 6 (4+8.5 RCC).

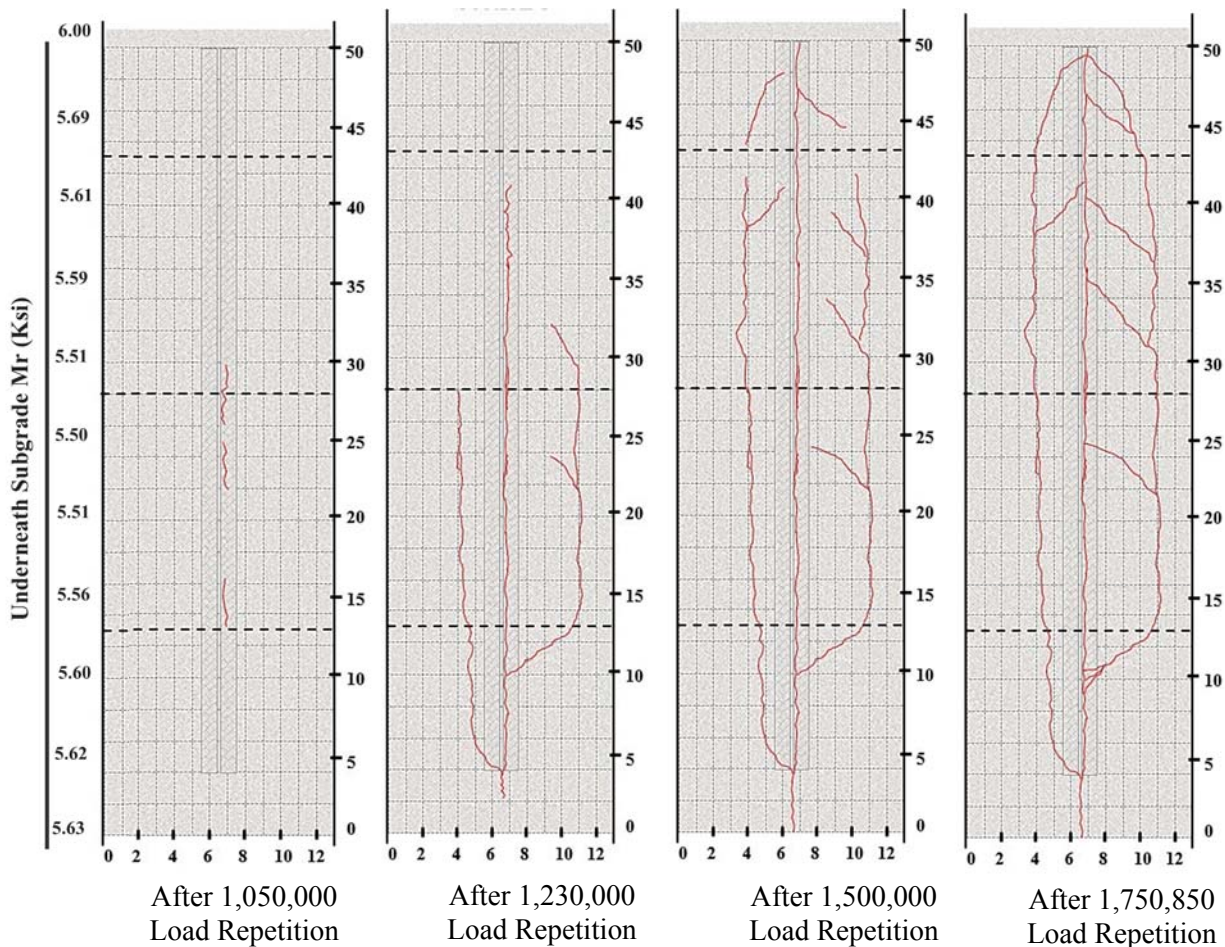


Figure 42
Cracks vs. load repetitions for Section 5 (6+8.5RCC)

The following findings may be observed from Figure 42: (1) the initial longitudinal cracking observed at the edge of a tire print seems to be a top-down fatigue cracking due to the high shear stresses under the tire wall; (2) the more uniform subgrade moduli resulted in a final cracking failure covering the entire loading area; (3) with continuous load repetitions and

pumping, voids could be formed underneath the 6-in. RCC slab, which generated more deflections and cracks of the slab under loading; (4) due to the combination factors of a thicker slab thickness, more uniform subgrade support and possibly high shear stresses under tire walls, the final cracking pattern of Section 5 (6+8.5RCC) was found much wider than that of Section 6 (4+8.5RCC); and (5) with a 2-in. increase in RCC thickness, the load carrying capacity of a RCC pavement could be significantly increased.



Figure 43
Distresses observed on Section 5 (6+8.5RCC)

Section 3 (4+12RCC)

Due to its relatively weaker support (the 12 in. cement treated soil is known to be weaker than the 8.5 in. soil cement built over the 10 in. cement treated subgrade), at the end of approximately 50,000 passes at 9kip of ATLaS dual tire loading, a longitudinal crack was observed along the wheel path, also in the middle of a tire print (showed in Figure 44) for Section 3 (4+12RCC).

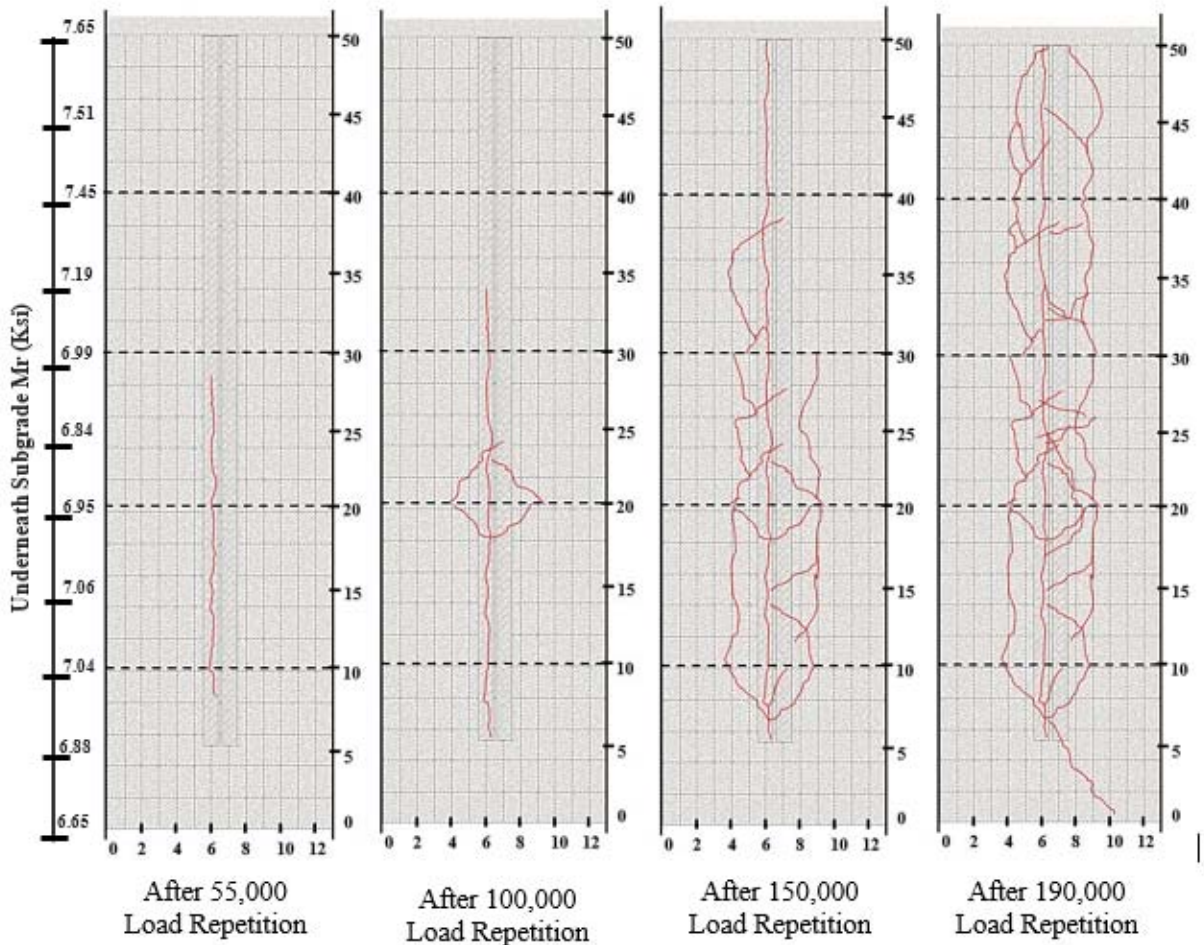


Figure 44
Cracks vs. load repetitions for Section 3 (4+12 RCC)

Section 2 (6+12RCC)

A total of 695,000 load repetitions of various loads were applied on this section and the estimated ESALs to the fatigue failure was 19.4 million. Figure 45 shows the cracking development under different load repetitions observed on Section 2 (6+12RCC). Similar to other sections, the crack was also initiated in longitudinal direction in this section and also the longitudinal cracking was initiated along the edge of a wheel tire similar to Section 5 (6+8.5RCC). It also showed that Section 2 with a 6-in. RCC over a weaker cement treated base may have a similar pavement life as Section 6 of a 4-in. RCC over a strong soil cement base.

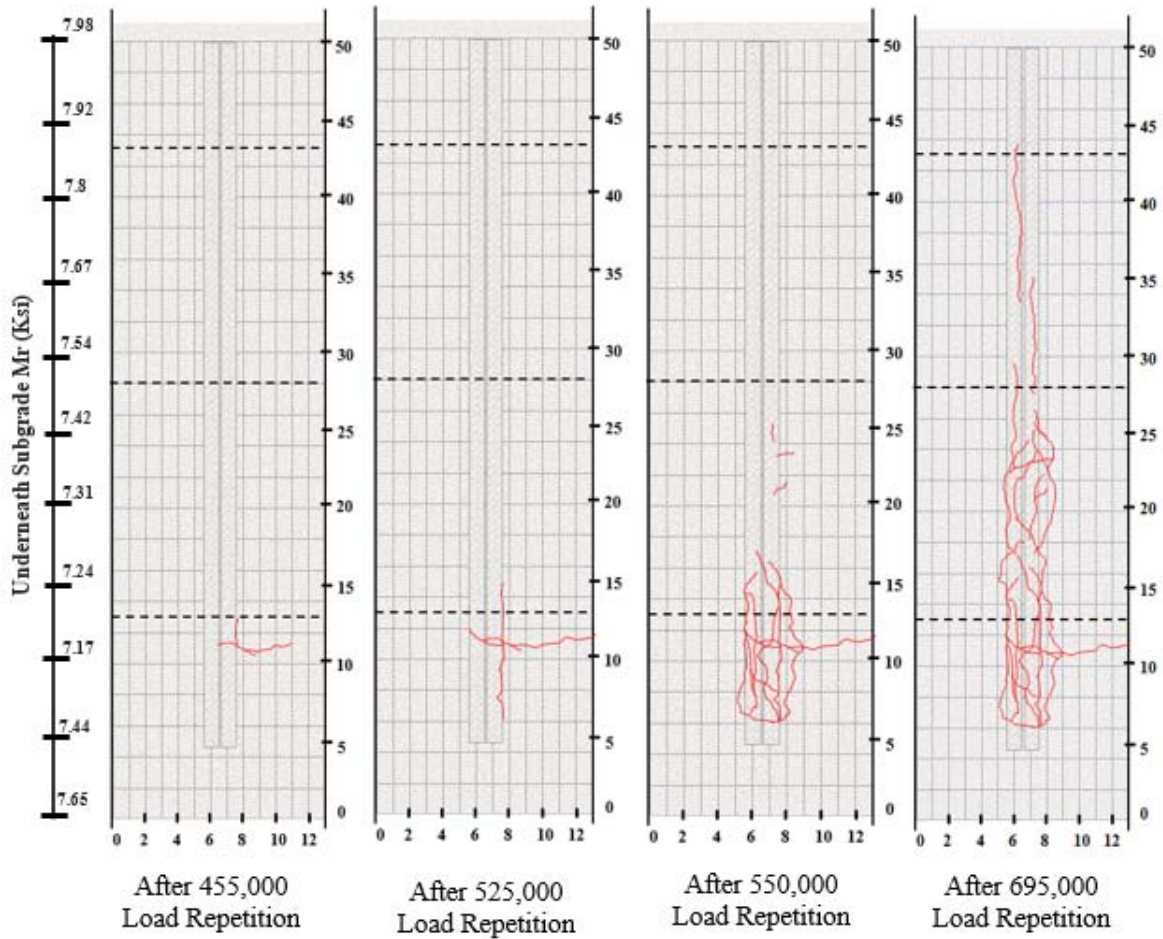


Figure 45
Cracks vs. load repetitions for Section 2 (6+12 RCC)

Section 4 (8+8.5RCC)

Only 392,500 load repetitions (approximately 11.3 million ESALs) were applied on Section 4 (8+8.5RCC). No significant damage was observed on this section. Due to the high load repetitions received on Section 5 (6+8.5RCC) to fatigue failure, the test was discontinued on Section 4 (8+8.5RCC).

APPENDIX B

STATE PROJECT NO: 30000682 / SPECIAL PROVISION

Amend Part VI, Rigid Pavement of the 2016 Louisiana Standard Specifications for Roads and Bridges with these supplemental specifications:

SECTION 603 ROLLER COMPACTED CONCRETE PAVEMENT

603.01 DESCRIPTION. This work includes constructing pavement or base composed of Roller Compacted Concrete (RCC) on a prepared subgrade or base course. Follow the requirements of these specifications and conform to the lines, grades, thickness, and cross-sections shown on the plans or as directed by the engineer.

603.02 MATERIALS Ensure that materials and methods meet the requirements of the following Sections and Subsections unless specified otherwise herein.

| | |
|--------------------------|--------------------|
| Portland Cement Concrete | 901 |
| Aggregates | 1003 |
| Joint Materials | 1005 |
| Curing Materials | 1011.01 |
| Water | 1018.01 |
| Asphalt Prime Coat | 505 |
| Admixtures | 901.08(b), 1011.02 |

(a) Aggregates. Use aggregates manufactured to meet the gradation at the quarry or blended at the plant site to produce the desired results. Use well-graded aggregates without gradation gaps and conform to the following gradation:

| Sieve Size | Percent Passing By Weight |
|------------------|---------------------------|
| 1 in (25 mm) | 100 |
| 3/4 in (19 mm) | 90 – 100 |
| 1/2 in (12.5 mm) | 70 – 90 |
| 3/8 in (9.5 mm) | 60 – 85 |
| No. 4 (4.75 mm) | 40 – 60 |
| No. 16 (1.18 mm) | 20 – 40 |
| No. 100 (150 µm) | 6 – 18 |
| No. 200 (75 µm) | 2 – 10 |

Produce evidence that the proportions have the capability for minimum strength development of 4000 psi (27.6 MPa) at 28 days and acceptable uniform gradation to attain specified density.

603.03 EQUIPMENT. Provide equipment and tools to construct RCC that will produce a completed pavement meeting the requirements for mixing, transporting, placing, compacting, finishing, and curing as provided in this specification. All equipment must be on hand and approved by the engineer before work can proceed. Comply with Sections 601 and 901 unless modified herein.

(a) Mixing Plant: Produce an RCC pavement mixture in the proportions defined by the approved mix design and within the specified tolerances. Capacity of the plant shall be sufficient to produce an uninterrupted uniform mixture at a rate compatible with the placement equipment. The mixing plant will be located within a 30 minutes' haul time from the RCC placement. With prior testing and the engineer's approval, use of a set retarding admixture is allowable to extend the haul time.

(1) Pugmill Plant: Pugmill plant shall be a central plant with a twin-shaft pugmill mixer, capable of batch or continuous mixing. Plant shall be equipped with synchronized metering devices and feeders to maintain the correct proportions of aggregates, cement, fly ash or slag, and water. The pugmill plant shall also meet the following:

(a) Aggregate Storage: If previously blended aggregate is furnished, storage may be in a stockpile fed directly to a conveyor-feeding mixer. For aggregate furnished in two or more size groups, provide aggregate separation at the stockpile.

(b) Aggregate Bins: Control feed rate by a variable speed belt or operate calibrated gate that accurately delivers any specified quantity of material. If two aggregate size stockpile sources are used, the feed rate from each bin shall be readily adjustable to change aggregate proportions, when required. Feed rate controls must maintain the established proportions of aggregate from each stockpile bin when the combined aggregate delivery is increased or decreased.

(c) Plant Scales: If used, any weigh box or hopper must be either a beam or a springless dial type, and be sensitive to 0.5% of the maximum load required. Provide beam-type scales that have a separate beam for each aggregate size, with a single telltale actuated for each beam, and a tare beam for balancing hopper. Belt scales will be of an approved design. Provide standard weights accurate to plus or minus 0.1% for checking plant scales.

(d) Cement, Fly Ash, or Slag Material Storage: Provide separate and independent storage silos for portland cement, fly ash, or slag. Identify clearly each silo to avoid confusion during silo loading.

(e) Cement, Fly Ash, or Slag Feed Unit: To assure a uniform and accurate quantity of cementitious materials enters the mixer, provide satisfactory means of dispensing portland cement, fly ash or slag, volumetrically or by weight.

(f) Water Control Unit: Measure by weight or volume the required amount of water for the approved mix. Equip the unit with an accurate metering device. Keep RCC mixture at optimum moisture by having the rate of water added adjustable.

(g) Gob/Surge Hopper: For continuous operating pugmills, attach a gob hopper to the end of the final discharge belt to temporarily hold the RCC discharge and allow the plant to operate continuously.

(2) Central Mix Batch Plant: Allowable for use in RCC work but must meet the requirements of Subsection 901.09.

(b) Paver: Place RCC with a high-density asphalt paver meeting the following requirements: Equip the paver with compacting devices capable of producing a RCC pavement with a minimum of 92% of the maximum wet density in accordance with AASHTO T-180, Method (D). Spread and finish the RCC material without segregation, to the required thickness, smoothness, surface texture, cross-section, and grade using a paver of suitable weight and stability.

Any alternative paving equipment must be approved by the engineer prior to use. The alternative paving equipment must spread and finish the RCC material without segregation, to the required thickness, smoothness, surface texture, cross-section, and grade without segregation, excessive tearing, or rock pockets.

(c) Compactors: For primary compaction, use self-propelled smooth steel drum vibratory rollers having minimum weight of 10 tons (9.07 Mg). For finish rolling as required for final compaction or for removing roller marks, use a steel drum roller, operating in static mode, a rubber tired roller or combination roller. For compacting areas inaccessible to large rollers, use walk-behind vibratory rollers or plate tampers.

(d) Haul Trucks: Provide sufficient number of trucks to ensure adequate and continuous supply of RCC material to paver. Equip trucks hauling RCC material from the plant to the paver with covers to protect the material from inclement weather and to reduce evaporation losses.

(e) Water Trucks: Throughout the paving and curing process, have at least one water truck or other similar equipment on-site and available. Equip the water truck with a spreader pipe containing fog nozzles capable of evenly applying a fine mist of water to the surface of the RCC without damaging the final surface.

603.04 Preparation. Prepare the subgrade or base course as required by the plans and Subsection 601.04 before placing the RCC. Ensure that the foundation immediately under the RCC pavement and the areas supporting the paving equipment will not contribute to deficient pavement thickness or excessive yield losses.

603.05 Construction Requirements.

(a) Submittals. Submit the following to the engineer at least 35 days before start of any production of RCC:

(1) Concrete Mix Design: Submit a mixture design prepared by a qualified testing laboratory. The engineer will transmit the design to the District Laboratory Engineer for approval. Include details on aggregate gradation, cementitious materials, admixtures (if used), compressive strengths (minimum 4000 psi), required moisture, density, and quantities of individual materials per cubic yard for the mixture design. Refer to ASTM C-1435, AASHTO T-22 (LA DOTD: TR-230M/TR-230-95) and AASHTO T-180 (Method D) for procedures. In addition to normal reporting requirement of AASHTO T-180 include curve calculations and graph.

(2) Paving Plan: Submit paving procedures: describing direction of paving operations, paving widths, planned longitudinal and transverse cold joints, curing methods, roller patterns, and description of all equipment.

(3) Trial Demonstration: The contractor shall validate the RCC mix design and paving plan with a complete trial demonstration. The contractor must demonstrate the proposed techniques of mixing, hauling, placing, compacting, finishing, curing, and preparation of the construction joints. Additionally, the test section provides the contractor the opportunity to demonstrate laydown method and rate, rolling pattern and method, and procedures for obtaining a density of not less than 98% of the maximum wet density in accordance with AASHTO T-180, Method (D). Construct the test section on an approved compacted base course using the same equipment, material, and construction techniques used on the ensuing work. The trial demonstration shall be of sufficient size to validate all the aspects of RCC paving including ability to achieve a smooth, hard, uniform surface free of

excessive tears, ridges, spalls, and loose material. The engineer may waive the trial demonstration if prior experience by the contractor using identical equipment, materials, and methods is acceptable to the engineer.

(b) Mixing Plant: Assure complete and uniform mixing of all ingredients. The volume of RCC material in the mixing chamber shall not exceed the manufacturer's rated capacity for dry concrete mixtures. Keep sides of the mixer and mixer blade surfaces free of hardened RCC and other materials. Check mixer blades routinely for wear and replace if wear is sufficient to cause inadequate mixing.

Ensure that mixing plant receives the quantities of individual ingredients to within the following tolerances: Cementitious Materials $\pm 2.0\%$, Water $\pm 3.0\%$, and Aggregates $\pm 4.0\%$

Prior to RCC production, provide a complete and comprehensive calibration of the plant in accordance to the standard specifications and certification requirements of the Department and manufacturer's recommendation. These calibration requirements will be waived by the engineer for those concrete plants currently approved and certified by the Department. Provide daily plant records of production and quantities of materials used that day to the engineer as required by the standard specifications.

(c) Transporting RCC: Transport RCC pavement material from the plant to the paver within 30 minutes as follows: Use dump trucks fitted with retractable protective covers for protection from inclement weather or excessive evaporation. Dump the trucks clean with no buildup or hanging of RCC material in the corners. Deposit the RCC material directly into the hopper of the paver or secondary distribution system that deposits the material into the paver hopper.

(d) Placing RCC: Keep subgrade or base course surfaces clean and free of foreign material and ponded water prior to RCC placement. Uniformly moisten subgrade or base course at the time of RCC placement. If the base course becomes dry, uniformly water, but the method of watering used shall not form mud or pools of freestanding water.

Adjust the paver and regulate the speed to prevent segregation and provide a surface course that is smooth and continuous, without tearing, pulling, or shoving. Limit the spread of the RCC to a length that can be compacted and finished within the appropriate time limit under the prevailing air temperature, wind, and climatic conditions. Proceed in a steady, continuous operation with minimal starts and stops. Regulate speed to assure a constant supply of RCC material in the hopper. Maintain RCC material above the auger shaft at all times during paving.

Place adjacent paving lanes within 60 minutes. If more than 60 minutes has elapsed

between placements of adjacent lanes, the vertical joint becomes a cold joint. Prepare the cold joint in accordance with “Cold Vertical Joints” as specified below. At the discretion of the engineer, this time may be increased or decreased depending on the use of set retarding admixtures or the ambient weather conditions of temperature, wind, and humidity.

Construct pavements greater than 10 in (250 mm) in two lifts of equal thickness; no lift shall be less than 4 in. (100 mm). For multiple lift placements, the thickness of each lift shall meet the requirements of “Lift Thickness” as follows. Place second lift within 60 minutes of the completion of the first lift. If more than 60 minutes has elapsed, the interface between the first and second lift is a cold joint. Prepare cold joint in accordance with “Horizontal Cold Lift Joints” as specified below. At the discretion of the engineer, this time may be increased or decreased depending on the use of set retarding admixtures or the ambient weather conditions of temperature, wind, and humidity. To reduce the opportunity for cold joints to develop, the use of multiple pavers in tandem formation is advantageous.

Limit use of hand spreading, broadcasting, or fanning to immediately behind the paver and before compaction. Remove any segregated coarse aggregate from the surface before compaction. If segregation occurs in the RCC during paving operations, cease the spreading until the cause is determined and corrected to the satisfaction of the engineer. If the engineer determines the segregation to be severe, remove and replace the segregated area at no additional cost to the Department.

Place RCC in a pattern so that any curing water from the previous placements will not pose a runoff problem on the fresh RCC surface or on the subgrade.

(e) Compacting: Begin compaction immediately after the placement of RCC material and complete within 60 minutes from the start of mixing at the plant. At the discretion of the engineer, this time may be increased or decreased depending on the use of set retarding admixtures or ambient weather conditions of temperature, wind, and humidity.

Plan operations and supply sufficient rollers to ensure specified compaction. Determine the sequence and number of passes by vibratory and non-vibratory rolling to obtain the specified density and surface finish. Do not operate rollers in the vibratory mode while stopped or reversing direction. Using rubber tire rollers for final compaction to knead and seal the surface is permissible. Do not operate roller within 12 in. (300 mm) of the edge of a freshly placed lane until the placement of adjacent lane. Within the allowable time, roll together both edges of the two lanes.

(f) Joints: For planned cold joints, roll the complete lane and follow cold joint procedures in accordance with “Cold Vertical Joints” below. Provide additional rolling for longitudinal joints with a vibratory roller as necessary to produce the specified density for the full depth

of the lift and provide a tight smooth transition across the joint. Smooth out any uneven marks left during the vibratory rolling utilizing a non-vibratory or rubber tire roller. Roll to obtain a smooth, flat surface, free of tearing and cracking. Avoid displacement of RCC pavement by optimizing the speed of the rollers at all times. Correct any displacement of RCC pavement resulting from reverse direction of the roller or from any other causes.

(1) Fresh Vertical Joints: Regard a vertical joint a fresh joint when an adjacent RCC lane is within 60 minutes of placement of the previous lane, with time adjusted depending on use of retarders or ambient weather conditions. Fresh joints will not require the treatment specified for cold joints. Construct joints to assure continuous bond between new and previously placed lanes.

(2) Cold Vertical Joints: *Note: Constructed vertical joints that use a drop extension or edging shoe are exempt from the following requirement when placed up to 15 degrees from vertical.* Cold joints are all construction joints in the RCC that do not qualify as fresh joints.

Treat longitudinal and transverse cold joints as follows: Cut the joint vertically full depth. Cut vertically at least 6 in. (150 mm) from the exposed edge. It is permissible to cut cold joints, cut within 2 hours of placing the RCC pavement, with approved mechanical equipment if no edge raveling occurs. Edges of cold joints cut after 2 hours of placing the RCC pavement, shall be saw cut to the full depth of the RCC pavement. Clean the joint of any loose or foreign material prior to placing fresh RCC material against a compacted cold vertical joint. Before placement of fresh RCC, wet the compacted cold joint to prevent excess loss of moisture.

(3) Fresh Horizontal Joints: For multi-layer construction, if placed within 60 minutes of placing the previous lift, a horizontal joint is a fresh joint; with time adjusted depending on use of retarders or ambient weather conditions. Clean the surface of all loose material and moisten the surface prior to placement of the subsequent lift.

(4) Horizontal Cold Lift Joints: For horizontal cold joints, clean all loose material and moisten the surface prior to placement of the subsequent lift. The plans or engineer may require use of a cement slurry or grout between lifts. If required, apply supplementary bonding materials immediately prior to placement, without loss of moisture, of the subsequent lift.

(5) Contraction Joints: RCC joint locations shall match existing joints in adjacent PCCP (shoulders) or as shown on the Plans or as directed by the engineer. Use early entry saws as soon as possible behind the rolling operation set to the manufacturer's recommendation. Saw cut contraction joints to a minimum of 1/4 depth of the compacted RCC pavement but no greater than 1/3 depth. Saw as soon as possible without causing

raveling or other damage to the pavement, but no later than 24 hours after placement.

(6) Joints at Structures: Treat joints between RCC pavement and concrete structures as cold vertical joints.

(g) Density: Perform in-place field density tests in accordance with TR-401, direct transmission, as soon as possible, but no later than 30 minutes after completion of rolling. Use wet density for evaluation. In-place field density shall be not less than 98% of the average maximum laboratory density obtained according to AASHTO T 180, Method D, based on the average of three consecutive tests per lot.

(h) Finishing: The finished surface of the RCC pavement shall meet the ride quality specifications set forth in 601.03.11 Surface Tolerance IRI.

(i) Curing: Immediately after final rolling and compaction testing, keep the surface of the RCC pavement continuously moist for 7 days or until an approved curing method is applied.

Water Cure: Apply water using water truck equipped with misting spray nozzles, soaking hoses, sprinkler system or other means that will assure a continuous and uniform moist condition to the RCC. Apply moisture in a manner that will not wash out or damage the surface of the finished RCC pavement.

Curing Compound: Apply curing compound, as specified in Subsection 601.10, in two separate applications at right angles to one another. After both passes, a minimum of 1 gallon per 100 square ft. is required. Ensure the application provides a uniform void-free continuous membrane across the entire RCC pavement surface.

Asphalt Prime Coat: If the final surface of the RCC is asphalt, place an asphalt prime coat in accordance with Section 505 to seal in the moisture of the RCC.

(j) Sealing Joints: Seal the joints in accordance with the plans and specifications or as directed by the engineer. Seal all RCC transverse contraction joints with material complying with section 1005.

(k) Permitting Traffic on Pavement: Before using the pavement as a haul road for loaded or unloaded vehicles, protect the RCC from vehicular traffic during the 7-day curing period or as approved by the engineer. Seal the joints before permitting vehicles or equipment on the pavement.

603.06 ACCEPTANCE REQUIREMENTS.

(a) General: There will be no direct pay from the Department for density and coring testing. Comply with Section 601.18 for acceptance requirements except as follows:

(1) Testing area/lot: 2000 square yards is the designated area for one lot.

(2) Compressive Strength for Mix Design Approval: Prepare and test 6 cylinders according to AASHTO T-180 (Method D) and AASHTO T-22 or TR-230 to determine the 28-day compressive strength. The Mix design will demonstrate a minimum compressive strength of 4000 psi (28 MPa) at 28 days.

(3) Density: For each lot, perform three random in-place field density tests in accordance with TR-401 using direct transmission and wet density for evaluation. Conduct tests as soon as possible, but no later than 30 minutes after completion of rolling. For full price payment, in-place field wet density shall be not less than 98% of the average maximum laboratory wet density obtained according to AASHTO T 180, Method D, based on the average of three consecutive tests per lot. Perform density tests within the middle third of the paved lane as viewed transversely.

(4) In-Place Concrete Strength Acceptance: RCC pavement lots not meeting the requirements outlined above, (3) Density, will be accepted at full price based on compressive strength development at 28 days of 3500 psi (25 MPa) or as stipulated in the payment adjustment schedule. For the circumstances where density requirements fail, obtain three cores, within the middle third of the paved lane as viewed transversely, for compressive strength testing in accordance with TR-225. For determination of diameter of cores (due to varying thicknesses of RCC), maintain an L/D ratio of 2.0 (core thickness / core diameter) as close as possible for best results in compressive strength testing. An L/D ratio greater than 1.25 is required. Saw cores with an L/D ratio greater than 2.0 to an L/D ratio of 2.0. *NOTE: transverse sawing of cores, for testing, may adversely affect the resulting compressive strength results.* For failure to meet density and minimum strength requirements, remove and replace the lot at the contractor's expense.

(5) Thickness: The average thickness of three cores per lot shall not be less the specified thickness by more than ½ in. The engineer will designate and evaluate areas deficient by more than 1/2 in (13 mm) thick. If the engineer requires removal, remove and replace the pavement in full-cross sections according to plan requirements. Removal and replacement will be at the contractor's expense.

603.07 MEASUREMENT.

Measure roller compacted concrete (RCC) for payment by the square yard (sq m). The quantities of roller compacted concrete measured for payment will be the design quantities

shown on the plans and adjustments thereto. Adjusted design quantities are if the engineer makes changes to adjust to field conditions, proven errors in the plans, or if design changes are necessary. Horizontal and longitudinal dimensions on the plans determine the design areas, the longitudinal length being along the centerline of the pavement.

603.08 PAYMENT.

Payment for Roller Compacted Concrete (RCC) pavement will be on a lot basis at the contract unit price per square yard (sq m), which includes all labor, materials, equipment, tools, testing, trial demonstrations, and any incidentals necessary to complete the work. Payment at the full contract unit price requires the tested lot achieves the 98-percent density requirements. For RCC pavement lots not meeting the 98% density requirements; acceptance is based on the following payment adjustment schedule for compressive strength development at 28 days.

Payment Adjustment Schedule (RCC)

| Compressive Strength, psi (MPa) | Percent of Contract Unit Price / Lot |
|---------------------------------|--------------------------------------|
| ≥ 3500 (24.1) | 100 |
| 3499 – 3300 (24.0 – 22.8) | 95 |
| 3299 – 3100 (22.7 – 21.3) | 85 |
| < 3099 (21.2) | 50 or Remove & Replace ¹ |

¹Remove and Replace at the option of the engineer after investigation and at the contractor’s expense.

Payment will be made under:

Payment items: **Item No. Pay Item Pay Unit**

NV-DEV-60301RCC Pavement ____in. (mm) Thick Square Yard (Sq m)

This public document is published at a total cost of \$250. 42 copies of this public document were published in this first printing at a cost of \$250. The total cost of all printings of this document including reprints is \$250. This document was published by Louisiana Transportation Research Center to report and publish research findings as required in R.S. 48:105. This material was duplicated in accordance with standards for printing by state agencies established pursuant to R.S. 43:31. Printing of this material was purchased in accordance with the provisions of Title 43 of the Louisiana Revised Statutes.